National Library of Canada
Acquisitions and Bibliographic Services Branch
395 Wellington Street
Ottawa, Ontario
K1A 0N4

Bibliothèque nationale du Canada
Direction des acquisitions et des services bibliographiques
395, rue Wellington
Ottawa (Ontario)
K1A 0N4

Your file Votre référence

Our file Notre référence

NOTICE

The quality of this microform is heavily dependent upon the quality of the original thesis submitted for microfilming. Every effort has been made to ensure the highest quality of reproduction possible.

If pages are missing, contact the university which granted the degree.

Some pages may have indistinct print especially if the original pages were typed with a poor typewriter ribbon or if the university sent us an inferior photocopy.

AVIS

La qualité de cette microforme dépend grandement de la qualité de la thèse soumise au microfilmage. Nous avons tout fait pour assurer une qualité supérieure de reproduction.

S'il manque des pages, veuillez communiquer avec l'université qui a conféré le grade.

La qualité d'impression de certaines pages peut laisser à désirer, surtout si les pages originales ont été dactylographiées à l'aide d'un ruban usé ou si l'université nous a fait parvenir une photocopie de qualité inférieure.

Canada

CISPLATIN RESISTANCE IN NONSMALL CELL LUNG CANCER: ROLE OF PLATINUM ACCUMULATION AND CELL MEMBRANES

By

Predrag Popovic

A thesis submitted to the
Faculty of Graduate Studies and Research
in partial fulfilment of the requirements
for the degree of

Master of Science

Department of Pharmacology, Faculty of Medicine

University of Ottawa
Ottawa, Ontario

July, 8, 1994

ISBN 0-612-00619-0

Canada

UNIVERSITÉ D'OTTAWA
UNIVERSITY OF OTTAWA

ABSTRACT

A cisplatin resistant cell line named E-8/0.7 was derived from the non small cell lung cancer HTB 56 cell line. According to IC_{50} estimations, E-8/0.7 cells were approximately 7.7 times more resistant to cisplatin than were HTB 56 cells.

Uptake of cisplatin 100 μM over 1 hour was measured by atomic absorption spectrophotometry, and showed around a 30 % lower uptake in E-8/0.7 cells compared to HTB 56 cells.

Barotropic behaviour was analyzed by pressure tuning infrared spectroscopy. In the CH symmetric stretching region, we found a lower break point (and consequently lower membrane fluidity) in E-8/0.7 cells compared to the parent cell line.

Lipid analyses of the two cell lines showed a higher cholesterol to phospholipid molar ratio in E-8/0.7 than in HTB 56 cells. Moreover, concentration of sphingomyelin was higher in E-8/0.7 cells than in HTB 56 cells.

ACKNOWLEDGEMENTS:

I would like to express my deepest appreciation to my thesis supervisor Dr. David Stewart. First of all, I would like to thank him for providing me the opportunity to do research in his laboratory and to have the benefit of his knowledge and experience. I also thank him for his advice, guidance, kindness and support.

I am grateful to Dr. Patrick Wong for allowing me to use highly advanced techniques in his laboratory. Moreover, I would like to thank him for encouragement, valuable explanations and discussions in interpretations of my results as well as tolerating my inexperience at the beginning of this project.

I wish to thank Dr Morris Kates for helping and overseeing me during analyses of cell lipids in his laboratory. His scientific knowledge, constructive criticism and patience are greatly appreciated.

My deep gratitude to Dr. Rakesh Goel for his valuable advice, encouragement and kindness throughout the duration of my training.

A special thanks to my colleagues from the pharmacology laboratory of the Ottawa Regional Cancer Centre: Dr. Matshela Molepo, Dr. Darshan Grewaal, Dr. Farshad Shirazi, Dr Ali Mohamed and Kevin Taylor for

their assistance, friendship and unforgettable hours spent with them.

I owe thanks to Doug Moffatt and Suzanne Lacelle from National Research Council of Canada and all the people from the physics laboratory at the Ottawa Regional Cancer Centre for their kindness and assistance.

Most importantly, I would like to thank those to whom this thesis is dedicated; my wife Biljana and sons Mihailo and Nikola for their support throughout this degree.

TABLE OF CONTENTS

LIST OF FIGURES

TABLES

LIST OF ABBREVIATIONS:

AA	Atomic Absorption
ATCC	American Type Culture Collection
$\delta_{as}CH_3$	Asymmetric Bending CH_3 Mode
$\delta_{s}CH_3$	Symmetric Bending CH_3 Mode
CDDP	Cisplatin (cis-diamminedichloroplatinum)
cm^{-1}	Wavenumber
DMSO	Dimethyl Sulfoxide
FCS	Fetal Calf Serum
GSH	Glutathione
GST	Glutathione S-Transferase
IMDM	Iscove's Modified Dulbeco's Medium
IR	Infrared (spectroscopy)
NSCLC	Non Small Cell Lung Cancer
PBS	Phosphate Buffered Saline
PC	Phospatidylcholine
PE	Phosphatidylethanolamine
PS	Phosphatidylserine
PTIS	Pressure Tuning Infrared Spectroscopy
SPH	Sphingomyelin
TLC	Thin Layer Chromatography
$\upsilon_{s}CH_2$	Symmetric CH_2 Stretching Mode
$\upsilon_{as}CH_2$	Asymmetric CH_2 Stretching Mode
$\upsilon_{as}PO_2^-$	Asymmetric Stretching Phosphate Mode
$\upsilon_{s}PO_2^-$	Symmetric Stretching Phosphate Mode

1.0 INTRODUCTION

1.1 Primary lung cancer

"A tumour is an abnormal mass of tissue, the growth of which exceeds, and is uncoordinated with, that of normal tissue, and persists in the same excessive manner after stimuli which evoked the change" (R. Willis's: Pathology of Tumours).

Lung cancer is the leading cause of cancer deaths in North America. Its incidence is rising steadily, especially among women. In Canada, more than 19000 new cases are estimated to have occurred in 1993. Lung cancer accounts for 20.5 % of cancer incidence, but causes 33.5 % of cancer deaths in males and 19.7 % in females, respectively. Only pancreatic cancer has a lower 5 year survival rate than lung cancer (Canadian Cancer Statistics 1993). Probability of developing lung cancer increases significantly with age. The main risk factors are: tobacco, asbestos,ionizing radiation (radon, therapeutic radiation) and heavy metals (nickel, chromium, iron oxides etc.). Lung scars, air pollution and genetic factors are also implicated, but the evidence for these etiologic factors is less conclusive

(Stauffer 1992). More than 20 types of benign and malignant primary neoplasms of the lung have been identified and classified histologically.

Primary malignant neoplasms are generally classified as either small cell carcinomas or non small cell lung carcinomas (NSCLC) (squamous cell, large cell and adenocarcinoma). Only 10-25% of lung cancers are asymptomatic at the time of diagnosis. In general, symptomatic lung cancer is advanced, and most often not resectable (Owens, Abeloff 1993). Diagnosis may be difficult, because physical findings vary and may be totally absent. Peripheral tumours (large cell carcinomas and adenocarcinomas) in particular may cause no abnormalities on physical examination. The prognosis for patients with NSCLC is poor. NSCLC accounts for 75 % of lung cancer cases, and less than 10 % are cured surgically. The median survival is less than 6 months for unresectable tumours and is 17 weeks with metastatic diseases (Rapp 1988). Prevention remains the major goal, but in spite of decreased smoking, lung cancer incidence continues to rise.

1.2 Current treatment for primary lung cancer

1.2.1 Surgery

Surgery remains the treatment of choice for patients with NSCLC. Unfortunately, surgery seldom is curative because of early dissemination of disease. After "curative" surgery of NSCLC, the 5 year survival rate is 35-40 % for squamous cell carcinoma and ~25 % for adenocarcinoma and large cell carcinoma (Stauffer 1992). Considerable efforts have been made to improve results of surgical treatment by postoperative adjuvant and preoperative neoadjuvant therapy, and studies underway should determine the value of neoadjuvant therapy.

1.2.2. Radiotherapy

Radiotherapy has shown some effectiveness in the palliative treatment of NSCLC. Moreover, it has been used as postoperative adjuvant and preoperative neoadjuvant therapy. Unfortunately, the doses that can

be delivered to tumours are limited by the tolerance of vital organs such as lung, heart, oesophagus, spinal cord and skin. Delayed damage of normal lung tissue ("radiation pneumonitis") is the major dose limiting complication. Radiation pneumonitis typically occurs 1-3 months after completing the therapy.

1.2.3. Chemotherapy

Chemotherapy has a role to play in NSCLC because of the very small number of patients that are cured surgically (less than 10 %) and the disappointing results of radiotherapy. A large number of single chemotherapeutic agents and multidrug regimens have been studied in clinical trials. Cisplatin is one of the most active drugs in the treatment of NSCLC, and the majority of chemotherapeutic regimens for NSCLC are cisplatin-based (Ginsburg et al. 1993, Dorr 1994).

1.3 CISPLATIN

1.3.1 Chemistry and mechanism of action

Cisplatin (cis-diamminedichloroplatinum), Pt(II) $(NH_3)_2Cl_2$ is an inorganic square, planar molecule (MW=300). The cis form possesses antitumour activity, whereas the trans isomer is virtually without antineoplastic activity. In cisplatin, the metal is in the + 2 state. The two chlorides in the molecule are stable at the relatively high (extracellular) concentration of chloride. Once inside the cell, the lower chloride concentration enables displacement of one or both chloride ligands for water or hydroxyl groups. This process creates highly reactive molecular species which can create stable bonds with DNA, RNA, proteins or other important cellular biomolecules. The NH_3 groups are kinetically inert, but they are important to the stability of the complex.

Cisplatin has a high affinity for $-NH_2$, -SH and COOH groups of amino acids. Binding to sulphur and nitrogen is strong, and dissociation is negligible under physiological conditions (Reed 1993).

Pressure Tuning Infrared Spectroscopic (PTIS) studies also revealed that high concentrations of cisplatin might disrupt protein intermolecular hydrogen bonds and might affect protein secondary structure (Popovic 1993). It appears that cisplatin reacts more extensively with RNA, than with DNA and proteins. Overall, cisplatin may produce multiple intracellular lesions, which can affect processes of transcription, translation and protein functions. It appears that enzymes are particulary sensitive to the influence of cisplatin (Reed and Kohn 1990).

Although, cisplatin's precise antitumour mechanism of action is still unclear, it has been widely accepted that cisplatin antineoplastic activity correlates with cisplatin-DNA interactions. It is believed that cisplatin induced DNA intrastrand cross linking is more responsible than interstrand cross linking for cisplatin antineoplastic activity (Reed 1993, Dorr 1994). Cisplatin can react with all DNA bases, but the N-7 positions of adenine and especially guanine are preferential binding sites. Approximately 60 % of total platinum binding to DNA takes the form of intrastrand dGpG diammineplatinum adducts (Reed and Kohn 1990).

Intramolecular hydrogen bonds between a proton of the cisplatin NH_3 group and oxygen of the DNA phosphate 5′ terminal stabilizes the complex. Platinum(II)-DNA interactions cause bending and consequent changes in the three dimensional conformation of DNA. There are some indications that DNA polymerase α is obstructed by cisplatin-DNA intrastrand GG adducts.

1.3.2 Cisplatin applications

Cisplatin antineoplastic activity was first reported in 1969 (Rosenberg et al.). Common indications for cisplatin use are: ovarian, testicular, bladder, lung and head and neck cancers (Ginsberg et al. 1993, Dorr 1994). Cisplatin is one of the most effective drugs in therapy of NSCLC, but not even cisplatin combinations give responses in all cases of NSCLC.

1.3.3 Mechanisms of cisplatin resistance

The major factor responsible for failure of cisplatin therapy is emergence of drug-resistant tumour cell populations. Although little is known about

mechanisms of resistance in vivo, a great number of studies have been done in vitro utilizing mainly cell lines and sometimes in vivo animal tumour lines that have acquired drug resistance in vitro. Those studies revealed that the main mechanisms of resistance can be grouped into three categories: 1) Changes in transmembrane transport of cisplatin, 2) altered cytosolic inactivation of the drug, and 3) increased DNA repair or increased tolerance to DNA damage (Johnson 1993, Doyle 1993). Moreover, altered folate metabolism, overexpression of some oncogenes and involvement of some membrane proteins and protein kinases A and C have been reported to be associated with cisplatin resistance (Scanlon 1989, Howell 1991).

1.3.4 Alteration of cisplatin transmembrane transport

Numerous investigators have reported positive correlations between cisplatin accumulation and cytotoxicity. The precise mechanism of cisplatin entry into the cell remains unknown. It has been widely accepted that cisplatin may enter cells by passive diffusion through the lipid bilayer (Mann 1988, Hospers

1988). That is supported by the observation that membrane disrupting agents can decrease or even reverse resistance (Morikage 1991), that cisplatin uptake is not inhibitable by cisplatin analogues and that cisplatin uptake does not occur against a concentration gradient. Some alternative cisplatin uptake mechanisms have also been suggested, such as active transport. In support of active transport are reports that drug accumulation is energy dependant, and is affected by membrane potential chnages resulting from altered activity of Na^+,K^+-ATPase (Andrews 1988, Andrews 1990). Decreased drug accumulation due to cell membrane changes can be caused by decreased influx or increased efflux. It has been shown that altered membrane composition may affect cisplatin accumulation (Timmer-Boscha 1989). There are also a few reports that some membrane glycoproteins are overexpressed in a cisplatin resistant cell line (Kawai 1990). One might speculate that those glycoproteins might have the same role as an energy dependant p-170 glycoprotein associated with resistance to several other antineoplastic drugs. However, conclusive evidence about this speculation has not been obtained. Hence, reduced cisplatin accumulation is an important mechanism of resistance and according to some reports it develops

early in cisplatin treatment, suggesting that this mechanism is primarily responsible for the ineffectiveness of cisplatin based chemotherapy.

1.3.5 Increased cisplatin inactivation

The cytosolic inactivation of cisplatin and consequent protection of DNA from the drug is the second pathway of drug resistance. Cisplatin is very reactive toward sulphydryl compounds. High glutathione (GSH) levels are associated with cisplatin resistance, especially with high levels of resistance. GSH is normally present in living cells, where it is involved in many detoxification processes and serves as a cofactor for many enzymes (Ozols 1993). On the other hand, depletion of GSH with buthionine sulfoximine (BSO), which irreversibly inactivates the enzyme γ-glutamylcystein synthetase, can increase sensitivity to cisplatin (Mistry 1991, Ozols 1993). In addition to nonenzymatic coupling, cisplatin's reaction with GSH may be catalysed by the enzyme glutathione S-transferase (GST). GST is a group of enzymes important for the

metabolism and detoxification of numerous endogenous and exogenous compounds. There are a few reports that elevated levels of GST and overexpression of the gene coding for GST (even without elevated GST activity) correlated positively with cisplatin resistance (Nakagawa 1988).

A group of sulfhydryl rich proteins (6000-7000 kDa), named metallothioneins, can also be important in cell defences against cisplatin (Scanlon 1989, Andrews 1990). Metallothioneins are composed of 30 % cysteine and they are very rich in thiol groups. Although most of the thiol groups are bound with Zn^{2+}, they are still capable of binding and inactivating cisplatin. High levels of metallothioneins can also protect cells against the toxic effects of some other heavy metals such as nickel, cadmium etc.

1.3.6 Increased DNA repair

Although approximately only 1 % of cisplatin inside a cell reacts with genomic DNA, it has been assumed that the DNA lesion is critical for cisplatin cytotoxicity (Behrens 1987). The evidence that best supports this

speculation is the observation that DNA repair-deficient cell lines have substantially augmented sensitivity to cisplatin. The most typical lesion caused by cisplatin is a DNA intrastrand cross-link between two adjacent guanines (Reed 1993). Additional types of lesions are those between neighbouring adenine and guanine bases and interstrand cross-links between two guanines separated by one or more bases (Reed 1993). However, the mechanism primarily responsible for cytotoxicity and antitumour activity has not yet been determined. Some reports emphasize inhibition of DNA replication caused by cisplatin, whereas others suggest apoptosis (due to DNA-cisplatin interactions) as a possible cause of cell death (Eastman 1990). Although the mechanism of repair of cisplatin-induced DNA damage is not clear yet, it appears that α and β polymerases might play important roles in DNA repair. In addition, recent studies showed that inhibitors of enzymes believed to be involved in DNA repair can modulate cisplatin cytotoxicity (Andrews 1990, O'Dwyer 1994).

1.4 Hypotheses and specific aims

We hypothesized that:

1. Cisplatin resistance is at least partly due to decreased cellular cisplatin accumulation.

2. Reduced cisplatin accumulation and cytotoxicity are accompanied by altered composition of cell membrane lipids.

The examination of these hypotheses was accomplished through:

1. Development of a cisplatin resistant subline by chronic exposure to cisplatin of the HTB 56 human lung adenocarcinoma cell line. The resistant cell line, named E-8/0.7, provided a very good model for further studies.

2. Measurement of sensitivity to cisplatin of HTB 56 and E-8 cell lines.

3. Measurement in both HTB 56 and E-8/0.7 cell lines of platinum accumulation (cellular platinum content) in early plateau phase, following exposure to 100 μM of cisplatin.

4. Analyses of pressure tuning infrared spectra of HTB 56 and E-8/0.7 cell lines.

5. Comparison of phospholipid composition and cholesterol content in HTB 56 and E-8/0.7 cells.

2.0 MATERIALS AND METHODS

2.1 Cell culture

Cells were cultivated and propagated by methods which are in routine use in the pharmacology laboratory of the Ottawa Regional Cancer Centre. All manipulations with cells were done in a laminar flow hood under sterile conditions. Cells were cultivated in Iscove's Modified Dulbeco's Medium (IMDM) (Gibco catalog # 380-2440 AJ), supplemented with 10 % heat-inactivated fetal calf serum (FCS), (Gibco catalog # 200-6140 AJ). Cells were subcultured from confluent flasks, usually between 4 and 6 days after seeding. Medium was aspirated and the cell monolayer was rinsed with 0.9 % NaCl or PBS (pH-7.4) to remove detached cells and cellular debris (which can affect cell counting). Trypsin was then added (1 ml for T-25 flasks and 2 ml for T-75 flasks). Cell monolayers were exposed to trypsin for 30 seconds and the trypsin was then removed from the flask. Trypsinized flasks were then incubated at 37°C for 2-3 minutes. Detached cells were resuspended in 5 ml IMDM medium, and an aliquot was taken for cell counting. Cells were counted by an electronic cell counter (Particle Data

Elzone 80) which had been calibrated by a haemocytometer.

Growth curves of both cell lines were obtained by seeding $5x10^4$ cells into 60 mm tissue culture dishes containing 5 ml IMDM medium. Cells from three plates were trypsinized and counted every 24 hours and the mean value was calculated. The growth curves of HTB 56 and E-8/0.7 cell lines are shown in figures 1 and 2. A bank of cell stocks was made by freezing a large number of cells ($\sim 3x10^6$) per cryovial. Cells from early plateau phase were trypsinized into single cell suspensions, pelleted by centrifugation, and supernatant was aspirated. Pellets were resuspended in IMDM medium containing 10 % v/v dimethyl sulfoxide (DMSO), transferred to cryovials, and stored at $-115^{\circ}C$. All experiments with both cell lines were performed with cells from early plateau phase. No antibiotics were used in any experiments.

2.2 Cisplatin treatment of the cells

An isotonic solution of cisplatin (1 mg/ml or 3.33 mM, pH 7.3) for clinical application was obtained from the pharmacy of the Ottawa Regional Cancer Centre. All experiments required lower drug concentrations, which were achieved by dilution of the clinical solution with isotonic saline (NaCl 9mg/ml). Cisplatin was applied directly into medium containing seeded cells. A maximum 50 µl of diluted drug stock solution was added by sterile micro-pipette to plates containing 5 ml IMDM medium.

2.3 Colony forming assay

The colony forming assay measures the ability of cells to form colonies following an experimental treatment. This method provides a good model system for chemotherapy where the goal is not only to kill malignant cells, but also to stop reproductivity and consequently tumour progression.

Cells were harvested from early plateau phase, (typically the fifth day) from T-25 flasks. A single

cell suspension was obtained as previously described (section 2.1). The suspension was diluted, cells were counted using an automatic cell counter, and an appropriate number of cells (~300) were seeded in 60 mm tissue culture plates containing 5 ml IMDM medium.

The plating efficiency was similar for both cell lines, and ranged from 35-52 %. Appropriate concentrations of cisplatin solutions were added at that time. Plates were left undisturbed in an incubator at 37°C humidified in a 5 % CO_2 atmosphere. After ten days, colonies were stained and fixed with crystal violet (0.2 % w/v in 70 % ethanol) for approximately 5 minutes. Excess stain was gently rinsed, the plates were dried and the colonies enumerated. The surviving colonies were counted under a binocular microscope at 10 x magnification. Only colonies containing more than 50 cells were taken into account. It was assumed that each colony originated from a single surviving cell which had attached to the growing surface and continued to divide. Colony forming assays were performed in triplicate at least four times for each cell line. Figures plotted are the mean percentage, with error bars representing standard error of the mean (SEM).

The degree of drug resistance was assessed by determining the 50 % inhibitory concentration for colony formation (IC_{50}) during the 10 day exposure. The percentage of surviving colonies was calculated according to the following formula:

$$\text{Surviving Fraction (\%)} = \frac{\text{mean \# of colonies in plates}}{\text{mean \# of colonies in control plates}} \times 100$$

2.4 Atomic Absorption Spectrophotometry

2.4.1 Background

When light of an appropriate wavelength hits an atom in its "ground state" (which is the most stable electronic configuration of an atom), the atom can absorb light and switch to a less stable configuration known as an "excited state". From the unstable "excited state", an atom will spontaneously return to its ground state. A displaced electron will quickly return to its previous orbital position, and radiant energy (the same as the energy of the absorbed light) will be emitted. This property of atoms to absorb light of a particular wavelength is utilized in atomic absorption spectrophotometry. This method measures the amount of light of a specific wavelength absorbed by an atom cloud. Free atoms are obtained by supplying enough thermal energy to disrupt chemical compounds into free atoms. The absorbency shows a linear relationship with concentration. Beer's law defines this relationship: A=abc, where "A" is absorbency, "a" is the absorption coefficient that is characteristic for the absorbing

species, "b" is the length of the light path, and "c" is the concentration of the absorbing substance.

Atomic absorption spectrophotometry has been evolving since 1960 when the first complete instrument was manufactured by Technotron (now Varian). In spite of many improvements, each atomic absorption apparatus must have a light source, a sample cell and detector. Because an atom absorbs light at a particular wavelength, it is very important to use a line source which emits a specific wavelength that can be absorbed by the atom of interest. Narrow line sources make this technique not only sensitive but also very specific. The most common line source is the "hollow cathode lamp", which was installed in the instrument used in this study.

The instrument can use a "single beam" where all measurements are based on changes in the intensity of that beam. In the "double beam" system, the sample beam is divided to create a reference beam directed around the sample to monitor lamp intensity. In the double beam system, the reading represents the ratio between the sample and reference beam. The recombined beam enters into a monochromator, where the light is dispersed and only the specific wavelength of interest is focused onto the detector.

The sample cell (i.e. the cell in which the sample is placed to be atomized) must provide conditions where atoms will be in their "ground state". In order to achieve that state, thermal energy must be applied, and most frequently this is accomplished by a flame. However, there is also flameless atomic absorption spectroscopy. The graphite furnace is a flameless sampling device which is currently the most advanced sampling technique. The heat required for atomization is provided by an electrical current which passes through the tube where the sample is placed. The sample is heated, with programmed temperatures for drying, ashing and atomization. Graphite furnace sampling has very high sensitivity, capable of detecting concentrations of ng/l for most elements (Gaffin 1979).

2.4.2 Sample preparation for AA spectrophotometry

Typically, 4-5 x 10^5 cells were seeded in 60 mm tissue culture dishes. When cells reached confluence, medium was aspirated and the cell monolayer was gently washed two times with PBS. Then 3 ml IMDM medium without FCS (warmed to 37°C) was added to the plates.

Cisplatin solution (90 µl, 100 µM) was then injected into each plate, and the plates were incubated at 37°C from 1 to 60 minutes. Time was very carefully measured. Following appropriate exposure times, medium was aspirated, and plates were rinsed 5 times in ice cold isotonic saline, left on ice for a couple of minutes and then scraped. Cells were scraped with a plastic policeman, and then were rinsed with 150 µl of PBS. Scraped cells were transferred to 2 ml Eppendorf tubes, and left at -20°C until analyzed (Mann 1990, Stewart 1994).

Before AA assay, the cell suspension was sonicated until a homogeneous suspension was obtained. The suspension was then vigorously vortexed for 30 seconds. A 20 µl aliquot of cell suspension was analyzed using a Varian Techtron AA-1475 spectrophotometer with a GTA-95 pyrolitically coated graphite tube. Every sample was assayed in triplicate. The graphite tube was cleaned after analysis of every third sample to remove contaminant deposits. Instrument calibration was done with three standards consisting of cisplatin (65.0, 162.5 and 325 µg/l) each day, before experiments were performed.

Absorbency was measured at 265.9 nm, with a slit width of 0.2 nm (Gaffin 1979). The temperature cycles of the graphite tube atomizer were:

Cycle	Temp. (°C)	Duration (sec.)
drying	95	50
ashing	1400	20
atomizing	2700	2.8

2.5 Protein assay

Concentration of cisplatin is expressed as pmol of platinum per mg of protein. Protein analyses were performed with the commercially available Bio-Rad Protein Assay based on the method of Bradford (Bradford, 1976). The principle of the method is based on a color changes of Brilliant Blue G-250 dye, which occurs in response to various concentrations of protein. The binding of the dye to proteins causes a shift in maximum absorption of the dye from 465 to 595 nm. Color development occurs after 2 minutes and remains stable

±4% for a period of 1 hour. Unlike other commonly used methods for protein determination (Lowry and biuret), this method is not affected by compounds such as potassium ion, magnesium ion, EDTA, thiol reagent, carbohydrates, ammonia etc. Scraped cells were homogenized by sonicator in Eppendorf tubes. Aliquots for protein assay (usually 50 µl) were kept with an equal volume of 1N NaOH for 24 hours. After that, 20 µl of digested sample was diluted with 80 µl PBS and 5 ml of dye (1:4 diluted and filtrated), mixed, and absorbency was read at 595 nm against a "blank" in a Philips UV/visible spectrophotometer, model PYE UNICAM PU 8610. Typically, five protein standards (10, 30, 50, 70 and 90 µg) were prepared with pure commercially available bovine serum albumin. The amount of protein was plotted against the corresponding absorbency, resulting in a standard curve (Bio-Rad protein assay manual).

2.6 Infrared Spectroscopy

2.6.1 Background

Infrared radiation promotes transition in a molecule between rotational and vibrational energy levels at the lowest ("ground") electronic energy state. Spectroscopy is the study of the interaction of electromagnetic radiation with matter. Infrared spectrophotometry measures the ability of matter to absorb, transmit or reflect infrared radiation. The infrared region of the electromagnetic spectrum lies between 0.8μ (microns) and 1 mm. By convention, band positions are expressed in wavenumbers υ (cm^{-1}). The relationship between wavelength λ (μm) and wavenumbers υ (cm^{-1}) is $\upsilon=10^4/\lambda$. The infrared spectrum is grouped into three regions: the far infrared from 200 cm^{-1} down to about 15 cm^{-1}, mid-infrared from 200 to 4000 cm^{-1} and near infrared from 4000 to 12500 cm^{-1} (Parker 1971).

In order to be infrared active, a dipole change during the vibration or rotation of the molecule must happen. If the molecule absorbs infrared radiation of the proper frequency and vibrational energy, in most

instances, rotation will be changed, and the affected molecule will rotate at higher frequency than before radiation was absorbed (Banwell 1972). That means that atoms will vibrate with a greater amplitude and bonds will be slightly elongated.

Homonuclear, diatomic molecules which do not posses dipole moments are non-polar. These molecules, such as O_2, N_2, H_2 etc., have an equal distance between the electron pairs that bind atoms into molecules. Consequently, they do not have dipole moments, and infrared radiation produces no changes in rotational or vibrational motions in those symmetric molecules. In heteronuclear molecules such as HCl, NO etc., atoms have different electron densities, and that unequal balance of charges is an electric dipole. Absorption of IR light causes a change in the electric dipole moment. IR techniques examine vibrational modes (type of vibrations) of molecules. Vibrations of isolated parts of the molecule result in different absorption bands. For example, an OH group in a molecule produces a particular absorption band which is observed in all molecules containing that group (Alpert 1972).

Spectral parameters such as frequencies, intensities, band widths and band shapes are used for

identification of substances (particularly organic compounds), determination of molecular structure, determination of purity, quantitative analyses, and reaction kinetic studies (Cross 1964). Moreover, spectral parameters have recently been successfully applied to cancer diagnosis (Wong 1990-1992).

2.6.2 Spectrophotometer

All IR instruments must posses some fundamental elements: a source of radiation, an optical system, a detector and an amplifier. The infrared radiation is typically produced by an electrically heated silicon carbide rod (called a Globar) or by a filament composed of zirconium, thorium and cerium oxides (called a Nernst glower) (Cross 1964).

The optical system must provide minimal loss of energy, because the infrared part of the electromagnetic spectrum is inherently low in energy. The beam is guided by silvered mirrors. Common lenses and mirrors are not used because of strong infrared absorption of glass. Windows are mostly made of mineral salts that are transparent to IR radiation, such as NaCl and KBr.

A monochromator serves to disperse IR light, and then only a narrow region of the spectrum is channelled through a slit to the detector. The detector function is to convert IR radiation into an electrical signal using its heating effect. Cooling the detector using liquid nitrogen improves its sensitivity. Two main types of detectors are in common use: thermal detectors and photon detectors based on photo-conductivity. An amplifier serves to amplify the low frequency signal to a level of many volts by several steps. Presently the alternating current amplifier is the preferred type.

2.6.3 Fourier Transform Infrared Spectroscopy

FTIR was originally developed for studies of the "far" infrared region. Improvements in computer techniques and engineering capabilities later allowed application of FTIR to other infrared regions. Basically, parallel infrared beams are directed to the beam splitter, which reflects 50% of the beam to two mirrors. Half of the radiation goes back through the same path, is recombined at the splitter, and is directed through a sample before reaching the detector.

One mirror is fixed, whereas the other moves smoothly toward and away from the splitter so the detector sees an alteration in radiation intensity, producing a curve of constructive and destructive interferences named interferograms. When the distances of the two mirrors from the splitter are equal, the two beams interfere constructively. If the moving mirror is displaced in either direction, then the two beams interfere destructively (Grim 1984, Smith 1979). The conversion of an interferogram to a typical spectrum (intensity versus frequency) is done by a mathematical process known as Fourier transformation. The main advantage of the FTIR instrument is its speed. With a computer connected to the instrument, many scans of the same sample can be taken and then averaged, consequently augmenting spectrum accuracy by improving the signal to noise ratio. Moreover, the resolving power is constant through the entire spectrum, whereas in prism instruments, the resolving power depends on the angle between the radiation beam and the prism, and this angle varies with frequency (Cross 1964, Alpert et al. 1970).

2.6.4 Pressure tuning Fourier-transform infrared spectroscopy

Pressure tuning infrared spectroscopy (PTIS) is defined as the study of pressure effects on vibrational spectroscopic features. Pressure distorts chemical bonds and intermolecular distances; therefore, weak molecular interactions at normal or low pressure may be substantially augmented at higher pressure. Addition of high pressure as a variable on spectral parameters such as frequency, band shape, intensity, and band splitting facilitates analysis of vibrational spectra. The instrument for PTIS must include a high pressure cell, which typically consists of a diamond anvil cell, figure 1 (Ferraro 1984). However, other materials can also be used for windows in high pressure cells, such as sapphire, glass, quartz, silicon etc. The advantages of diamond are: i) the pressure can be increased up to 100 kbar; ii) the type IIa diamond used for the mid-infrared region absorbs very little in that region; iii) a small amount of liquid or solid sample can be analyzed, (typically 0.1 mg); iv) the sample may be examined unprocessed in its natural state.

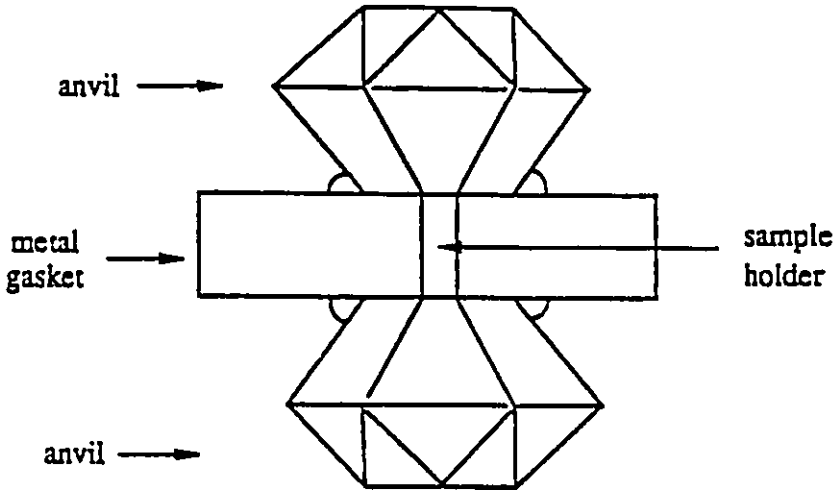

Figure 1: Opposed diamond anvil cell

There are also some disadvantages of opposed diamond cells. The diamond may absorb in the region of interest (2000-2500 cm^{-1}); however, other materials which do not absorb in that region can be used over a limited pressure range from 6 to 13 kbars. Using two high-pressure cells, one equipped with diamond windows and the other with sapphire windows, spectral regions from 400-4000 cm-1 can be fully covered.

The source beam in some instruments is focused to a 1 cm diameter, while the diameter of the gasket hole is about 0.3 cm; therefore, a beam condenser is required. Finally, large amounts of sample cannot be analyzed (Mantch 1990).

The amount of pressure exerted on the sample is determined from the 695 cm^{-1} infrared band of α quartz, which is used as an internal calibrant (Wong 1985). The equation for pressure calculation using the phonon band of α quartz is:

$$P(kbar) = 0.1516\Delta v^2 + 1.2062\ \Delta v^2$$

In the equation, P is pressure and Δv is the frequency shift in cm^{-1} compared to the frequency at atmospheric pressure.

PTIS has been used in studies of structural and dynamic properties of molecular systems in the solid and liquid states, as well as in solutions. Moreover, relatively recent PTIS methodological and technological advances have allowed successful studies of very complicated biological systems. PTIS has been used in studies of human tissues, isolated cells and cellular macromolecules (RNA, DNA, lipids and proteins) (Wong 1987, Goral 1990).

Raw data were converted into DOS by software obtained from the manufacturer. Data were then processed by software developed at the National Research Council of Canada by Doug Moffat.

2.6.5 Sample preparation for PTIS

HTB 56 and E-8/0.7 cells were cultivated as previously described in section 1.5.1. Cells in early plateau phase from 2-3 T 75 flasks were washed three times with PBS or isotonic saline and harvested mostly by gentle scraping, although sometimes trypsinization was used. Control experiments did not reveal any changes in spectra caused by the method of harvesting. Detached cells were resuspended in 8-10 ml PBS, then spun down at 4°C. Supernatant was aspirated and the cell pellet was again resuspended in 2 ml of PBS, transferred to an Eppendorf tube, and centrifuged at 800 x g for 5 minutes. The pellet in the Eppendorf tube was stored at -115°C until analyzed.

2.7 Analyses of cell lipids

Cells from 2-3 square plates in early plateau phase were harvested by scraping. Typically, the volume of the cell pellet used for extraction was 1 - 1.5 cm^3. Lipid analyses of HTB 56 and E-8/0.7 cells were performed at the same time under the same experimental conditions.

2.7.1 Extraction of total lipids

During this procedure, lipids are isolated in an undegraded form, free of water soluble substances such as sugars and amino acids. Extracting solvents (polar and non-polar) disrupt Van der Waals, hydrogen and electrostatic bonds between lipids and proteins. However, covalently bound lipids cannot be extracted by solvent. They must be cleaved from mainly polysaccharides etc., by acid or alkaline hydrolysis.

To extract total lipids we used the method described by Bligh and Dyer, later modified (Kates 1986). Briefly, into a wet cell paste were added chloroform and methanol, to make a chloroform-methanol-water solvent system (1 : 2 : 0.8, v/v), assuming the

cell pellet to be equivalent to water. The mixture was vigorously vortexed and left at room temperature for 1 hour. The supernatant was transferred to a 50 ml glass stoppered graduated tube. This procedure was repeated two more times and the supernatants were combined. To these combined supernatants, chloroform and water (1 : 1, v/v) were added, making a final chloroform-methanol-water ratio (1 : 1 : 0.9). This created a two phase system. All water soluble particles were readily dissolved in the upper methanol-water phase, whereas lipids stayed relatively free of contaminants in the lower chloroform phase. The solution was centrifuged, and the chloroform phase was aspirated by Pasteur pipet. Two more times chloroform was added to the water-methanol phase and the procedure was repeated. The combined chloroform phases were put in a 250 ml round bottom flask, diluted with benzene (to remove traces of water) and evaporated to dryness in a rotary evaporator. The round bottom flask was then put in a desiccator under vacuum. The round bottom flask was weighed empty and again after chloroform distillation on an analytical balance, to determine the total lipid weight. The lipid residue was then dissolved with chloroform, making sure that the walls of the round bottom flask were thoroughly

rinsed and brought to a known volume (typically 10 ml). Part of this 10 ml stock solution was diluted, and an aliquot from that solution was used for determination of total cholesterol and total phosphorus.

2.7.2 Analyses of major phospholipid classes

2.7.2.1 Background

Phospholipids are biochemical compounds that contain hydrophillic and hydrophobic sections. They can be divided into glycero-phospholipids and sphingolipids. The backbone of phospholipids is a glycerol. A phosphate group is bound to the glycerol and an organic group (choline, ethanolamine, serine etc.) is bound to the phosphate group, making together a phosphatidyl head group which is hydrophillic. The hydrophobic section of the phospholipid is composed of two fatty acids attached to the glycerol backbone. The nomenclature of phospholipids takes into account the fatty acids and the head group.

For example in 1-palmytoil-2-oleoyl-sn-glycero-phosphocholine, 1-palmytoil and 2-oleoyl refer to

particular fatty acids, whereas phosphatidyl choline describes the head group (Stryer 1988). In the lipid bilayer, the phospholipid head groups are located outward and the fatty acid tails are inward. As many as 40 different fatty acids may be incorporated into sn-1 and sn-2 positions of phospholipid molecules.

Phospholipids are like detergents: when placed in water above a critical temperature they will spontaneously form bilayer structures. This membrane-forming process is driven by non polar interactions of the fatty acid chains. The interactions of the polar head groups are repulsive. Both, the attractive interactions of fatty acid chains and repulsive interactions of polar head groups are essential for maintenance of the lipid bilayer (Boggs 1987).

Phospholipids mainly exist in cell membranes in the form of separate domains, and are asymmetrically distributed in the lipid bilayer (Klausner 1980, Bevers 1989). For example, in human red blood cells, phosphatidyl choline and sphingomyelin are located in the outer leaflet, whereas phosphatidyl ethanolamine and phosphatidyl serine are in the inner leaflet (Emmelot 1975). The abundance of particular phospholipids in a cell depends on the cell type and cell organelles. For

example mitochondria are rich in cardiolipin, and nerve cells are rich in phosphatidyl serine (Robert 1983). Cell membrane phospholipid composition and cholesterol content are carefully regulated by the cell, depending on cell cycle, age, various stimuli and changes in environment. Phospholipids provide the basic structure and the permeability barrier of cellular membranes. Moreover, they are major source of cellular second messengers and are also important for activity of membrane bound enzymes (Sanderman Jr 1978, Soderberg 1991).

2.7.2.2 One dimensional thin layer chromatography

One dimensional thin layer chromatography is very effective in the separation of polar lipids. Commercially available 20 cm x 20 cm Whatman silica gel plates were used (Fisher Cat. # 05-713-171). Silica gel is a slightly acidic substance with a pore diameter between 6 and 15 nm, supported by glass plates. All plates used in the experiments were first washed with chloroform-methanol (1 : 1, v/v) prior activation at 120^{o}C for 30 minutes. One third of the plate was used

for standards, whereas sample was applied on the other 2/3 of the plate. For quantitative analysis, about 4-5 mg of lipids were dissolved in 300-400 µl of chloroform and applied 2 cm from the bottom of the plate using a streaker with microsyringe.

The solvent system used for separation of major phospholipid classes was chloroform-methanol-concentrated ammonium hydroxide (65 : 35 : 5, v/v) (Rouser 1976). The chromatographic development tank was lined with filter papers, to provide a solvent-saturated atmosphere, and the lid was sealed with masking tape to prevent loss of solvent vapour. Two plates containing samples from HTB 56 and E-8/0.7 cells were placed in the chromatography tank at the same time. After solvent migration 1.5 cm up to the top, plates were removed and dried in a fume hood for ~10 minutes under a stream of nitrogen. Plates were then put in a covered tank with an excess of iodine crystals at the bottom and left for a few minutes until brownish spots developed. Spots were outlined with pencil before the color disappeared (Kates 1986). The identification of the spots from samples was determined by comparison to location of standards run under the same experimental conditions.

2.7.3 Phosphorus analysis

The outlined spots of major phospholipid classes on the TLC plates (including at least one blank) were carefully scraped and transferred to 20 ml screw-capped (teflon linen) tubes. Immediately 4.5 ml of 0.6 N methanolic-HCl was added to each tube, and the tubes were heated for 2 hours. For sphingomyelin assays, heating was for 5 hours instead of 2 hours in 4.5 ml of 2 N methanolic-HCl (Kates 1986). After cooling, 0.5 ml of distilled water was added, and methyl esters of fatty acids were extracted with 3 portions (5, 4 and 3 ml) of petroleum ether. Combined portions were left in a cold room at 4°C for later analysis by gas-liquid chromatography. In some cases, suitable aliquots of internal standard (17:0) for fatty acids were added before methanolysis, while in others methyl esters of 17:0 fatty acids were added after methanolysis.

The bottom methanolic-water phase was vigorously vortexed, centrifuged at 1500 x g for 2 minutes, and the supernatant was transferred to a 10 ml volumetric flask. This procedure was repeated three more times with 2, 2 and 1 ml of methanol. Supernatants were combined and were brought to a 10 ml volume by adding methanol.

Blanks were treated in the same manner as the phospholipid samples.

Quantitative estimation of phospholipids requires the obligatory step of the conversion of organic into inorganic phosphorous. The colorimetric determination of phosphorous is a very sensitive method, and can give erroneously high values of phosphorous. Hence, all glassware must be thoroughly washed with chromic acid-sulphuric acid. In this study, Lewis-Benedict sugar tubes in which phosphorous was to be determined were kept in chromic acid-sulphuric acid overnight. Just before use they were thoroughly rinsed with distilled water, dried in the oven for a few minutes and covered with beakers treated in the same way. In spite of careful, thorough cleaning in this manner, a very deep blue color sometimes developed, indicating dirty tubes, and the experiment had to be repeated.

Suitable aliquots from the methanolic phase (containing head polar groups of phospholipids) were taken and transferred into Pyrex straight walled Lewis-Benedict sugar tubes containing glass beads. Solvent was then evaporated completely. Samples were then digested with 0.4 ml 70 % perchloric acid in a Kjeldah digestion rack heated electrically until samples became colourless

(typically 4-5 minutes). After cooling, samples were diluted with 4.2 ml of distilled water, 0.2 ml of 5 % ammonium molybdate (w/v), and 0.2 ml freshly prepared amidol solution (0.25 g 2,4-diaminophenol dihydro chloride and 5 g sodium metabisulfite in 25 ml of distilled water). Tubes were vortexed, covered with small beakers, and put in boiling water for 7 minutes to allow development of stable blue color. After 15 minutes, absorbency was read at 830 nm in a 1 cm diameter cuvette against a reagent blank in a Philips SP 8-500 UV-visible spectrophotometer. For calibration 1, 2 and 4 µg of phosphorous standards were carried simultaneously through the procedure, but without digestion. Beer's law is valid up to 10 µg phosphorous. Phosphorous concentrations in samples were determined according to the following calculation: µg P in a sample aliquot = absorbency of sample x (µg P in standard)/ (absorbency of standard).

It should be noted that the P value obtained from the "blank" was accordingly subtracted from P values obtained from the phospholipid spots (Kates 1986).

2.7.4 Cholesterol assay

Aliquots for cholesterol analysis were taken from diluted stock solutions at the same time as aliquots for total phosphorous determination. The chemical method used for total cholesterol analysis generally showed good reproducibility. Sample aliquots in chloroform (containing up to 300 µg of cholesterol) were placed in test tubes and evaporated to dryness under a stream of nitrogen. To the samples were then added 3 ml of glacial acetic acid and 2 ml of color reagent. Color reagent was prepared by dissolving 0.5 g of $FeCl_3 \cdot 6H_2O$ in 20 ml concentrated (85%) orthophosphoric acid. The 2 ml of that solution was diluted in a volumetric flask up to 25 ml with concentrated H_2SO_4. After cooling, light yellow color developed (Kates 1986). Solutions were vortexed, cooled (10 minutes), and absorbency was read at 550 nm against a reagent blank in a Philips SP 8 - 500 UV visible spectrophotometer. A standard curve was prepared with 25, 50, 100 and 200 µg of cholesterol. Beer's law is valid up to 500 µg of cholesterol. Samples were analyzed in duplicates or triplicates. When readings of concentration were outside the calibration range, dilutions were made and the samples were reanalysed.

3.0 RESULTS

3.1 Establishment of cisplatin resistant cell line

The purpose of this experiment was to provide a good model system with which to study the mechanism(s) of cisplatin resistance. The HTB 56 cell line was chosen for this study because of its relatively high sensitivity to cisplatin in comparison to other NSCLC cell lines (which possess intrinsic resistance). The HTB 56 cell line was isolated in 1976 by J. Fogh, and can be obtained from the American Type Culture Collection (ATCC) (Rockville, U.S.A.).

The HTB 56 cell line was isolated from a 61 year old female caucasian treated with radiation. It is an anaplastic carcinoma with features of adenocarcinoma in the nude mouse and in vitro (ATCC catalogue 1991).

Cisplatin resistance was established using a modification of a previously described procedure (Hong 1988). All cell lines were maintained as a monolayer in antibiotic-free medium. Plateau phase cells from T-25 flasks were used in this experiment. Approximately 10-15 cells were seeded in a 96 well flat-bottomed microtest

plate. Wells contained 250 µl of IMDM medium with an appropriate amount of cisplatin.

HTB 56 cells were initially exposed to 0.2 µg/ml of cisplatin and kept in an incubator until large colonies appeared in a few wells after 2-4 weeks, these colonies were trypsinized and propagated further. The first week after removal from the well, cells were maintained in T-25 flasks in a medium without cisplatin, following 5-6 weeks maintenance in medium containing cisplatin. Cells from the E-8 well showed the highest vitality, and were continued in culture and were treated with progressively higher doses of cisplatin. The same cloning procedure was than repeated using progressively higher cisplatin doses (0.5, 0.7 and 1.5 µg/ml) leading to the development of the resistant E-8/0.5, E-8/0.7 and E-8/1.5 sublines. Subsequent experiments with resistant sublines were done after culturing cells at least 10-14 days in cisplatin free medium.

3.2 Cisplatin cytotoxicity in HTB 56 and E-8/0.7 cells

Plateau phase cells harvested from T-25 flasks were used for determination of the relative cytotoxicity of cisplatin. Approximately 300 cells were seeded in 5 ml of IMDM medium in 60 mm tissue culture dishes as described in section 2.3. Cisplatin concentrations of 0, 0.05, 0.075, 0.1, 0.15, 0.2, 0.3, 0.4, 0.5, 0.6, 0.7, 0.8, 0.9 and 1.0 µg/ml were used. After 10 days of undisturbed exposure, colonies were processed and counted as described in section 2.3.

Dose response curves of HTB 56 and E-8/0.7 cell lines are shown in figure 2. Each point on the curves represents an average of at least three independent experiments performed in triplicate. The cell survival vs concentration was not linear: the steepest slope was observed between 0.1 and 0.2 µg/ml in HTB 56 cells, whereas in E-8 cells the steepest slope was between 0.7 and 0.8 µg/ml. In addition, there was a considerable shoulder on the E-8/0.7 dose response curve in the 0-0.4 µg/ml range. This shoulder could be possibly explained by acquired mechanisms of resistance, as described in sections 1.3.3 - 1.3.6. The concentrations of cisplatin required for 50% inhibition of colony formation of the

HTB 56 and E-8/0.7 were 0.09 and 0.7 µg/ml, respectively (figure 2 and table 2). Periodic repetitions of IC_{50} determinations of the resistant variant maintained in a medium containing 0.7 µg/ml of cisplatin revealed a small gradual increase in the degree of cisplatin resistance over a period of 10 months. Maintenance of the E-8/0.7 cell line in cisplatin-free medium for more than two months did not affect the degree of resistance, indicating that stable genetic changes had probably occurred.

Dose response curves of the HTB 56 cell line and its resistant variants are shown in (figure 3). Most of the studies were performed on the E-8/0.7 variant although some preliminary studies were done on E-8/0.5 and E-8/1.5.

The dose response curve of E-8/1.5 cells was not presented because only one experiment in triplicate was performed, which indicated a high degree of resistance and substantially decreased plating efficiency of E-8/1.5 cells. In the colony formation assay, plating efficiency (percentage of cells plated, giving colonies) was slightly lower for E-8/0.7 cells than for HTB 56 cell, ~53.4% vs ~47.8% (table 2).

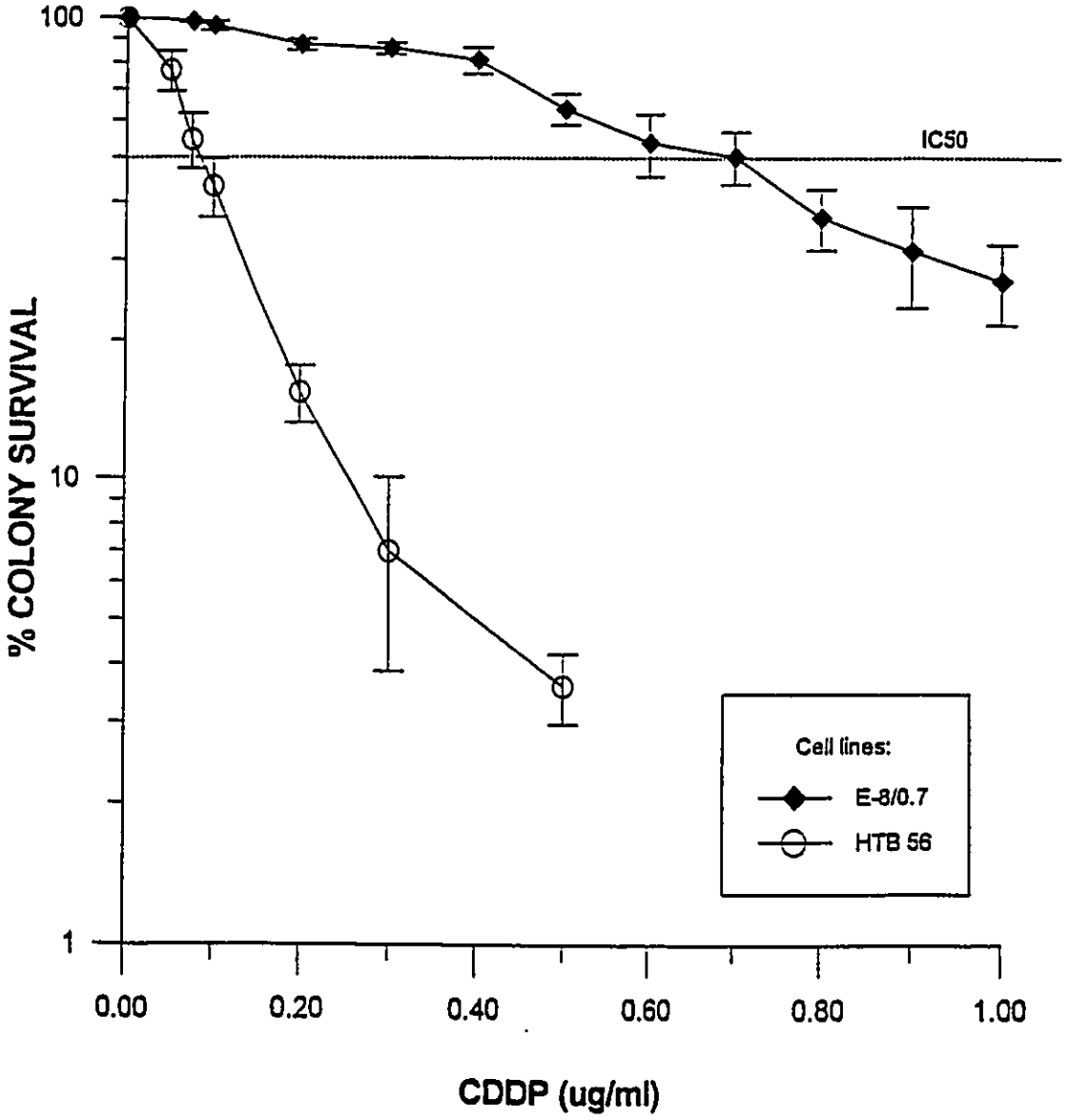

Figure 2: Dose response curves for cisplatin determined by the colony forming assay (prolonged exposure, 10 days). Points and bars represent mean ± SEM.

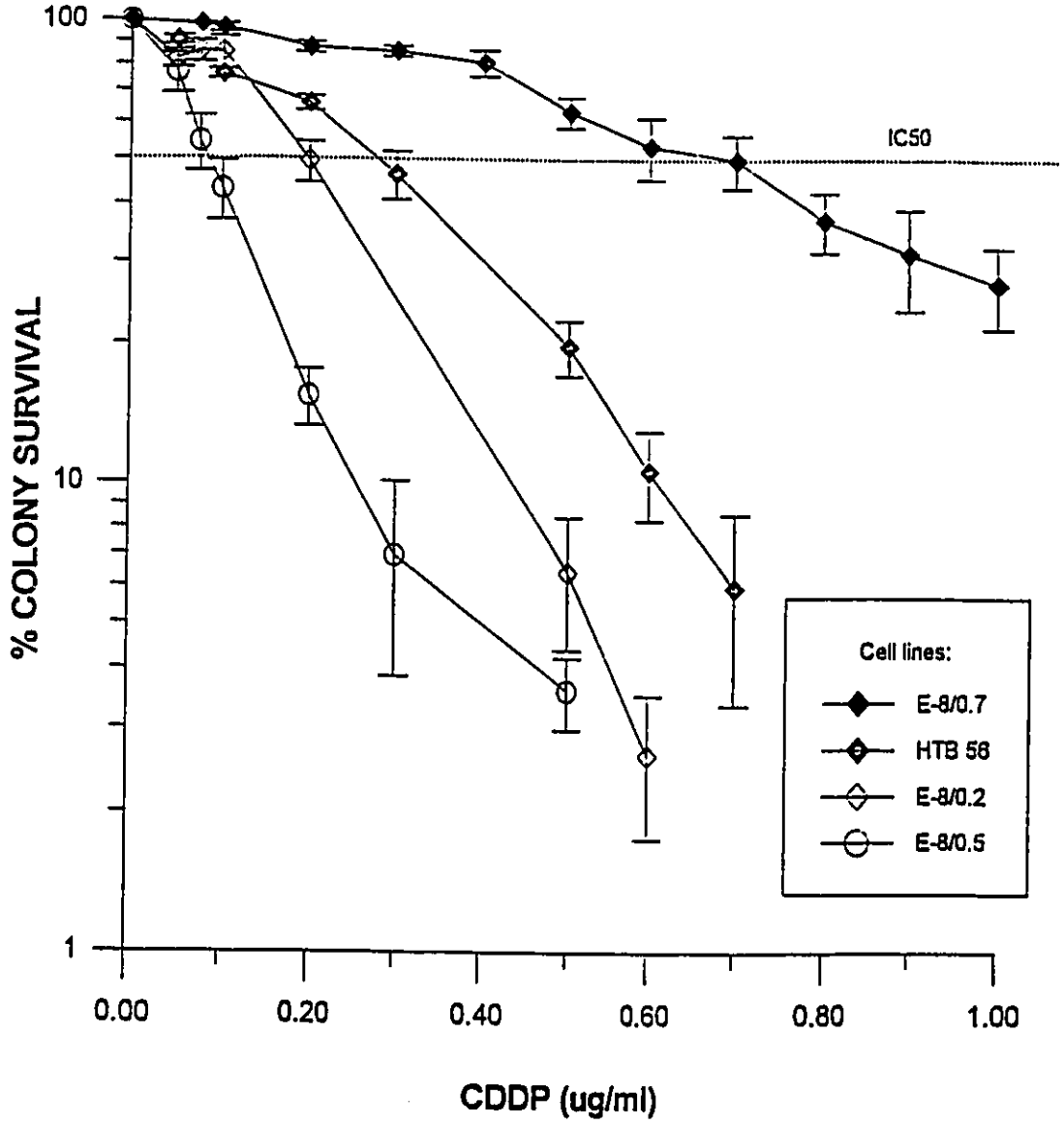

Figure 3: Dose response curves for cisplatin of the HTB 56 cells and its resistant variants, assessed by colony forming assay. Points represent mean ± SEM.

The growth curves presented in figure 4. show that resistant cells replicate more slowly than do HTB 56 cells, which do not have a lag phase. Cell population doubling times calculated from the exponential part of the growth curves were approximately 21.4 hours for HTB 56 cells and 26.4 hours for E-8/0.7 cells. This finding is similar to selected other reports indicating that growth capacity is diminished in resistant sublines (Kikuchi 1986, Hong 1988, Hospers 1990). However some other authors have reported comparable doubling times in parent cell lines and their resistant variants (Teicher 1987), or even an increase of doubling time in the parent cell line (Behrens 1987). Hence, cell growth rate and resistance are probably not intrinsically linked. E-8/0.7 cells took one day longer to enter the exponential growth phase than did HTB 56 cells. The number of HTB 56 cells reached a plateau on the fourth day, whereas E-8/0.7 cells reached a plateau on the fifth day. Once cells reached a plateau and the monolayer became overconfluent, cells started to lift off the plate.

Microscopic observation of E-8/0.7 cells showed morphological changes (increase in cell size and bizarre elongated shape) when exposed to cisplatin (0.7 µg/ml),

which disappeared after a few days of maintaining cells in a medium without cisplatin.

Electron microscopic morphological and structural changes induced with cisplatin in fibrosarcoma and glioma cell lines have been reported: cell rounding, a reduced nuclear-cytoplasmatic ratio, clumping of nuclear chromatin, vesiculation and swelling of golgi apparatus and dilatation of the smooth endoplasmatic reticulum (Oberc-Greenwood 1990). It should be emphasized that these morphological changes were observed after exposure of cells to high, clinically irrelevant doses of cisplatin. Table 1 shows the relative resistance to cisplatin of some sublines reported in the literature. According to data in this table our E-8/0.7 cell line can be categorized as having a moderate or even low degree of resistance. Table 2 summarizes some characteristics of HTB 56 and E-8/0.7 cell lines.

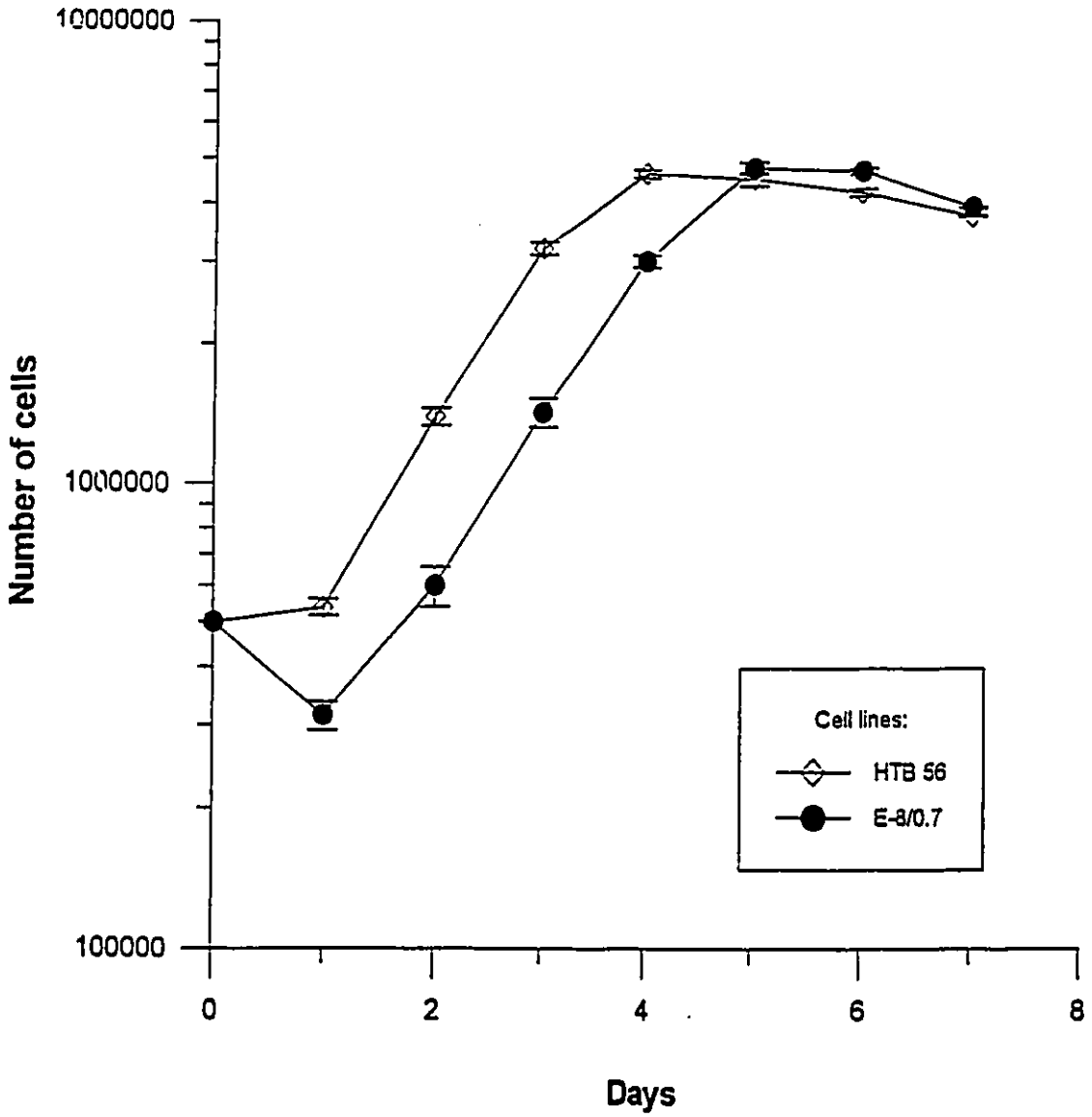

Figure 4: Growth curves

TABLE 1 RELATIVE CISPLATIN RESISTANCE OF VARIOUS CELL LINES

CELL LINE	TUMOUR TYPE	RESISTANCE*	REFERENCE
KFr	ovarian	20	Kikuchi 1986
2780^{cp8}	ovarian	7.3	Behrens 1987
2780^{cp20}	ovarian	14.0	Behrens 1987
2780^{cp70}	ovarian	39	Behrens 1987
$L1210/DDP_{10}$	murine leukemia	110	Richon 1987
SCC-25/CP	SCLC	30	Teicher 1987
2008/DDP	ovarian	2.4	Andrews 1988
MCF-7/CDDP	breast	6.5	Frei III 1988
PC-7/1.2	NSCLC	22.9	Hong 1988
PC-14/1.5	NSCLC	3.1	Hong 1988
PC-9/0.5	NSCLC	7.1	Hong 1988
GLC-4/CP	SCLC	11	Timmer Boscha 1989
PC-9/CDDP	NSCLC	28	Fujiwara 1990
H69/CPR	SCLC	8.8	Twentyman 1992
MOR/CPR	NSCLC	3.5	Twentyman 1992
L23/CPR	NSCLC	4.3	Twentyman 1992
GCT27cisR	testicular	5.6	Kelland 1992
PC10-B3	NSCLC	11.4	Katambi 1992
PC10-E5	NSCLC	19.9	Katambi 1992
Tera-CP	embryonal	3.7	Timmer Boscha 1993

Table 1-Continued

CELL LINE	TUMOUR TYPE	RESISTANCE	REFERENCE
2780/DDP	ovarian	7.7	Schmidt 1993
HCT/DDP	ovarian	1.6	Schmidt 1993
RL2	rat colon	6	Oldenburg 1994
RL4	rat colon	20	Oldenburg 1994
E-8/0.7	NSCLC	7.7	Popovic 1994

* Resistance was mainly determined according to IC_{50} assessment, although in a couple of cases, IC_{90}'s were used for determination of the degree of resistance.

3.3 Cell size determination

This experiment was conducted on an "Elzone" electronic particle counter equipped with a channelizer, manufactured by Particle Data Inc. Cells were suspended in special electrolyte which must be virtually free of particles for accurate particle size analysis. Cells in a non conductive material go through a small orifice essentially singly along with electric current. This causes electric pulses, dependent on flow velocity, orifice size and cell concentration. Pulse amplitudes positively correlate with the volume of the particles. For routine usage, diameters of the orifices range from 12 to 1200 μm, with a total measurable span of 0.15-900 μm. The orifice diameter is selected to be 50-100% greater than the biggest particle. Particle size data acquisition and processing were done by software purchased from the manufacturer (Karuhn 1984).

The size of cells in the E-8/0.7 resistant subline was slightly larger than that of the parent HTB 56 cell line, but this difference did not achieve statistical significance (table 2). The sizes of HTB 56 and E-8/0.7 cells were 11.64$\pm$1.4 μm and 12.16$\pm$0.4 μm respectively.

CHARACTERISTICS OF THE HTB 56 AND E-8/0.7 HUMAN LUNG ADENOCARCINOMA CELL LINES

Table 2

CHARACTERISTICS	HTB 56	E-8/0.7
CISPLATIN IC_{50}	0.09 µg/ml	0.7 µg/ml
RELATIVE RESISTANCE*	1	7.7
DOUBLING TIME (h)	21.4±0.6	26.4±1.0
PLATING EFFICIENCY (%)	~53.4	~48.7
CELL SIZE (µm)	11.64±1.4	12.16±0.4

* Relative resistance = IC_{50}-resistant subline/IC_{50} parent cell line

3.4 PTIS analysis of HTB 56 and E-8/0.7 cells

Infrared spectroscopy has been used increasingly in recent years for studies of cells and tissues (Benedetti 1990, Rigas 1990, Le Gal 1991, Wong 1991[a&c] etc.). In general, cells contain small molecules (up to 50 atoms) and polymers that are composed of small molecules (monomers) linked together. Fourier-Transform Infrared spectroscopy of cells records vibrations of macromolecules (polymers) such as nucleic acids, proteins, lipids and carbohydrates.

Spectral bands were studied between 900-1700 wavenumbers (cm^{-1}) and between 2800-3000 cm^{-1}. These two regions are most commonly used in the study of biological systems (Dev 1984, Goral 1990, Wong 1991[a]).

Figures 5 and 6 show a stacked plot of HTB 56 and E-8/0.7 cells up to a pressure of 9 kbar, while figure 7 illustrates pairs of representative infrared spectra of both cell lines at the same low pressure. It is evident from figures 5-7 that spectra of these two cell lines are very similar. Observed peaks belong mainly to the vibrational modes of functional groups of cellular macromolecules.

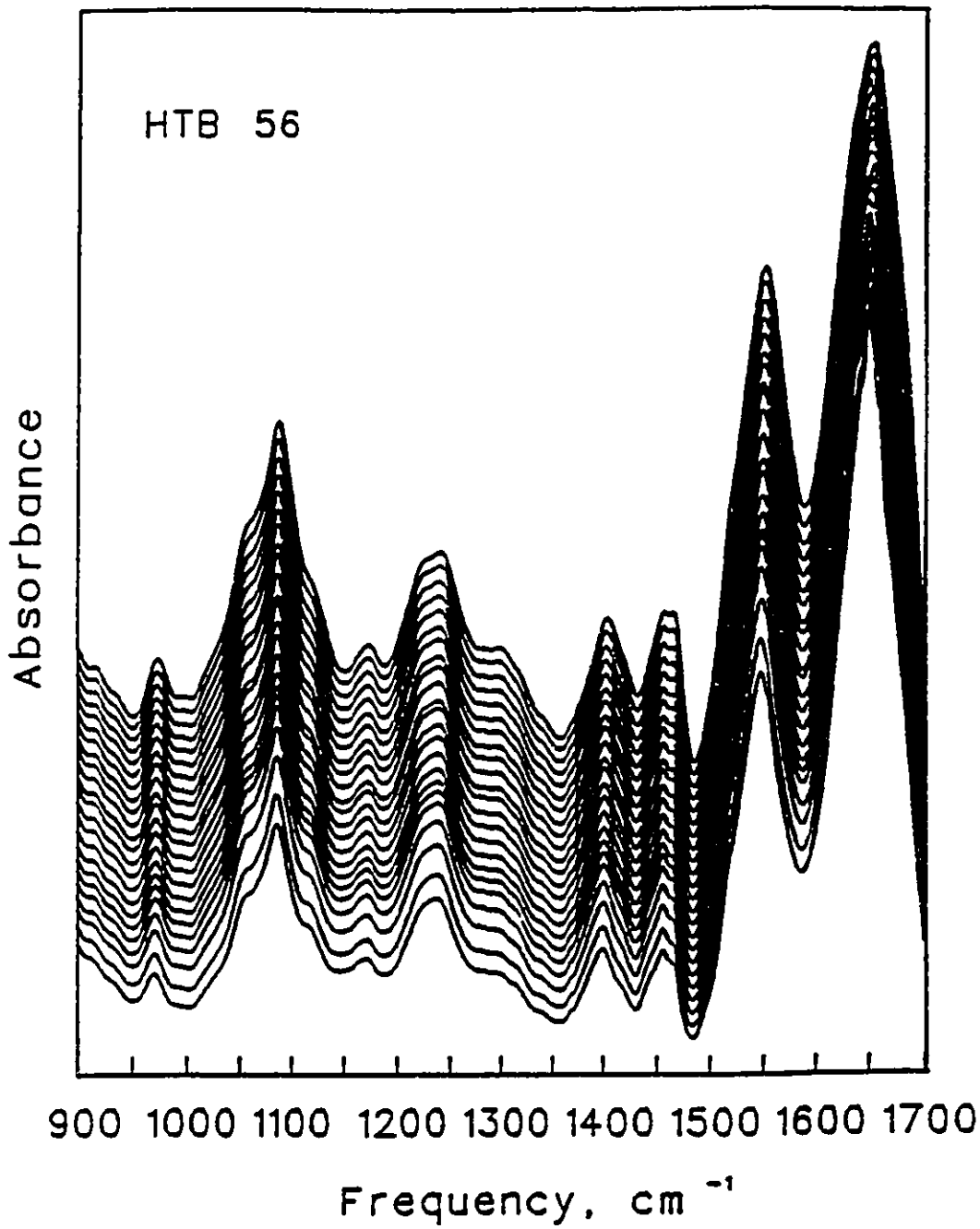

Figure 5: Stacked contour plots (absorbance vs frequency vs pressure [up to 10 kbar]) of infrared spectra of HTB 56 cells in the frequency region 900-1700 cm^{-1}. The top contour plot represents the spectrum at the highest pressure tested (~10 kbar).

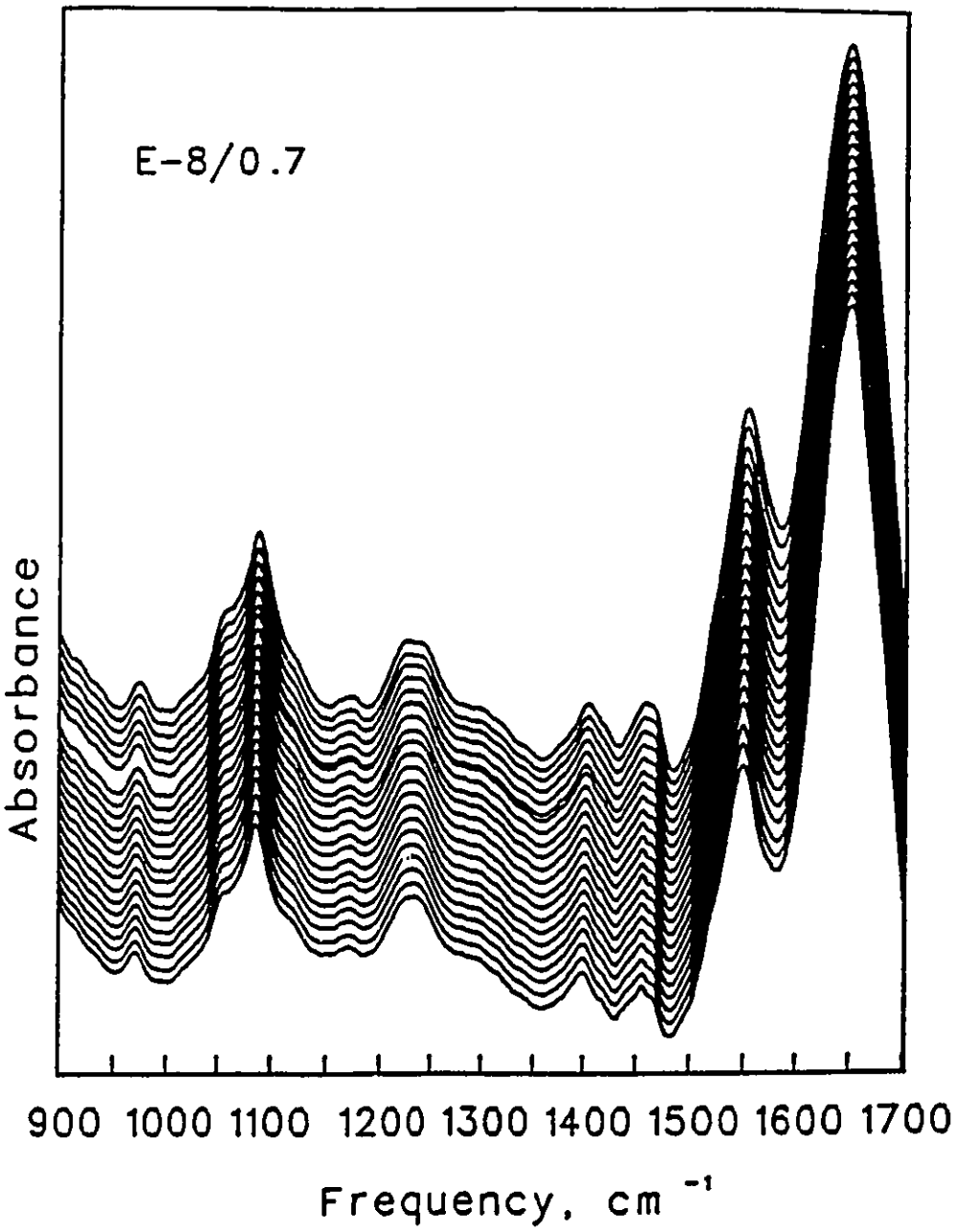

Figure 6: Stacked contour plots (absorbance vs frequency vs pressure [up to 10 kbar]) of infrared spectra of E-8/0.7 cells in the frequency region 900-1700 cm^{-1}. The top contour plot represents the spectrum at the highest pressure tested (~10 kbar).

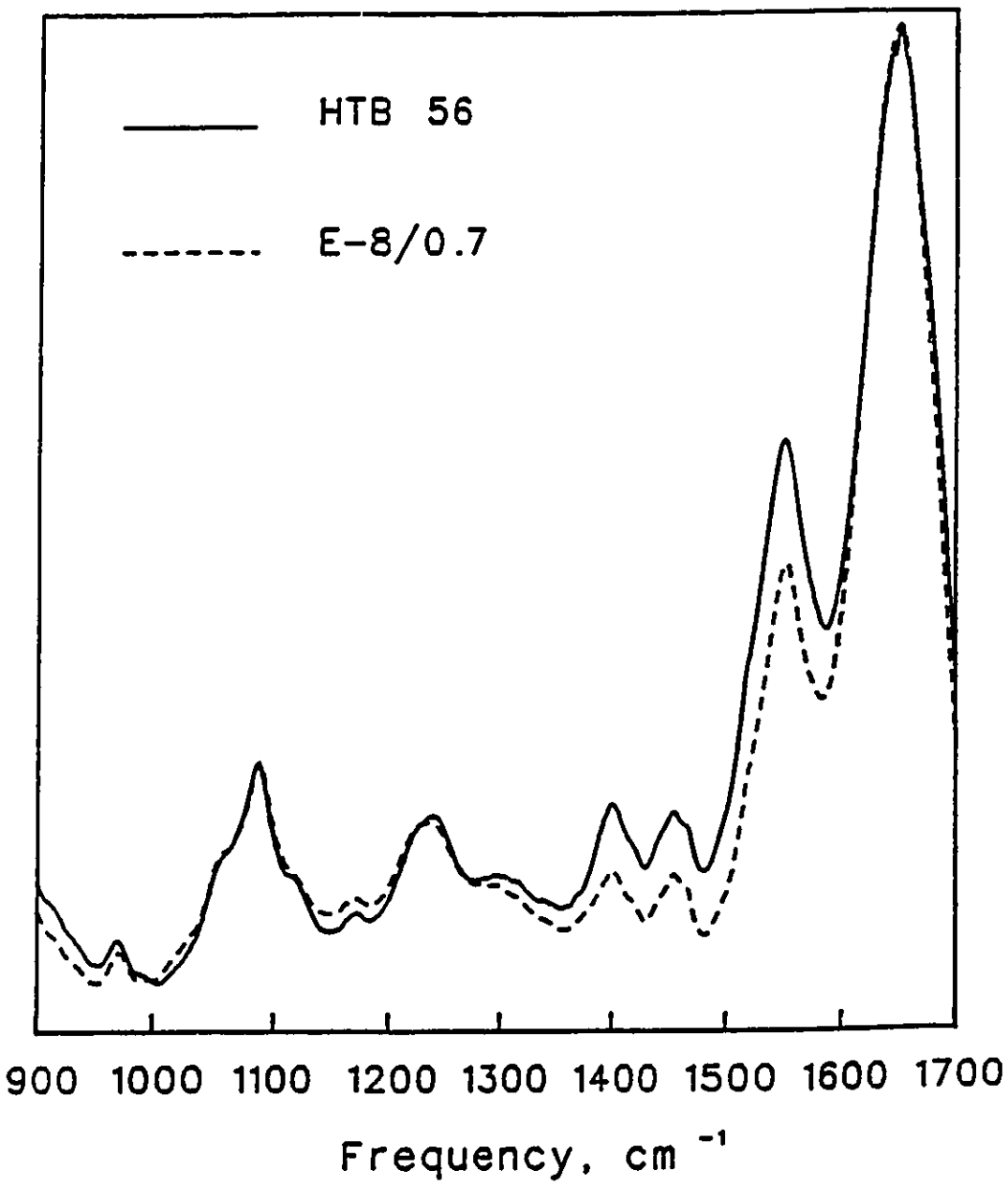

Figure 7: Representative infrared spectra of HTB 56 and E-8/0.7 cells in the frequency region 900-1700 cm^{-1}.

The peak around 970 cm^{-1} is due to the symmetric stretching vibrations of dianionic phosphate monoesters of phosphorylated proteins and cellular nucleic acids (Sanchez-Ruiz 1988, Wong 1991[c]). The peaks at ~1086 cm^{-1} and 1240 cm^{-1} are mainly due to symmetric ($\upsilon_s PO_2^-$) and asymmetric ($\upsilon_{as} PO_2^-$) phosphate stretching modes respectively of cellular nucleic acids (Parker 1971, Shie 1972). Contribution of phospholipids and other compounds that contain phosphodiester groups to the intensity of these bands is negligible (Wong 1991[b], Wong 1991[c]).

The C-O stretching band ~1170 cm^{-1} is mainly due to stretching vibrations of C-OH groups of serine, threonine and tyrosine amino acids of cellular proteins (Rigas 1990, Wong 1991). The peaks ~1400 cm^{-1} and 1458 cm^{-1} originate mainly from symmetric ($\delta_s CH_3$) and asymmetric ($\delta_{as} CH_3$) bending modes of cellular proteins (Parker 1971, Wong 1991[c]). The weak band ("shoulder") ~1467 cm^{-1} originates from CH_2 bending frequencies of the methylene chains in lipids (Wong 1987, Mantch 1988, Philp 1990).

The bands ~1550 cm^{-1} and ~1650 cm^{-1} are amide II and amide I bands originating from vibrations of amide groups in cell proteins (Susi 1969, Parker 1971, Dev

1984). The other important bands investigated in this study were in the CH stretching region (2800-3000 cm^{-1}). The peaks ~2852 cm^{-1} and ~2920 cm^{-1} arise from CH_2 symmetric ($\upsilon_s CH_2$) and asymmetric ($\upsilon_{as} CH_2$) stretching modes, respectively, of the acyl chain methylene groups (Casal 1984, Wong 1987, Siminovitch 1987). Two other bands observed in that region are ~2958 cm^{-1} and ~2874 cm^{-1}. These latter two bands are due to symmetric ($\upsilon_s CH_3$) and asymmetric ($\upsilon_{as} CH_3$) stretching modes of the methyl groups from cell proteins and terminal CH_3 groups of acyl chains. Therefore, cell proteins and lipids contribute to the intensity of these bands (Parker 1971, Rigas 1990).

Figures 8, 9, 10 and 11 indicate that basically there are no differences detectable by PTIS between HTB 56 and E-8/0.7 cells in the spectral regions that belong to nucleic acids. Figure 10 and 11 show the asymmetric phosphate stretching band in HTB 56 and E-8/0.7 cells. The $\upsilon_{as} PO_2^-$ band consists of two overlapping bands around 1220 cm^{-1} and 1240 cm^{-1}. The lower frequency band is due to hydrogen bonded phosphodiester groups, whereas the higher frequency band is due to non-hydrogen bonded phosphodiester groups (Rigas 1990, Wong 1991[b]). Although, the deconvoluted spectra at the bottom of

figure 10 show slightly higher absorbency in E-8/0.7 cells than HTB 56 cells, this difference is not considered to be important.

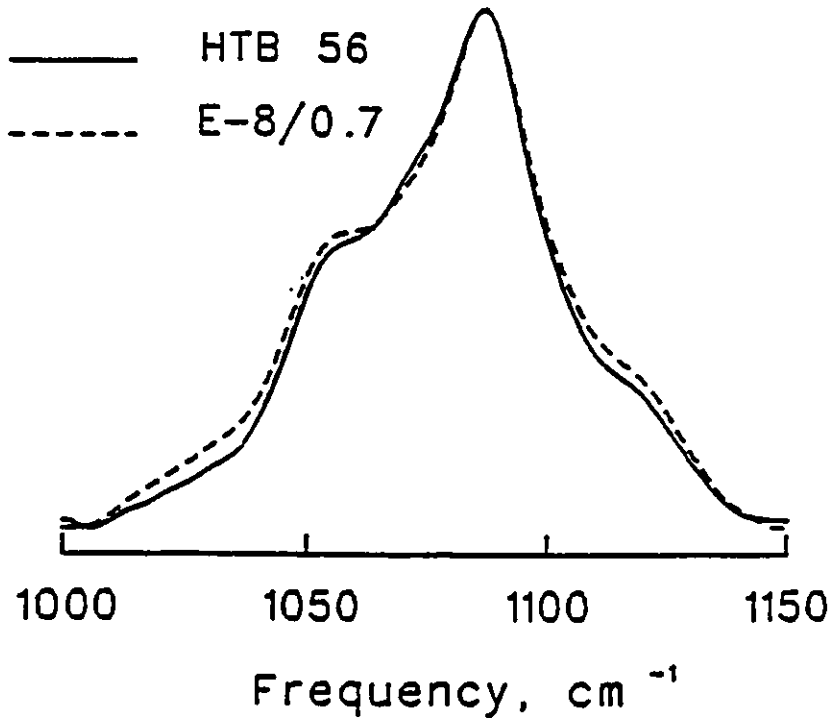

Figure 8: Representative infrared spectra of the HTB 56 and E-8/0.7 cells in the symmetric phosphate stretching region at comparable pressures.

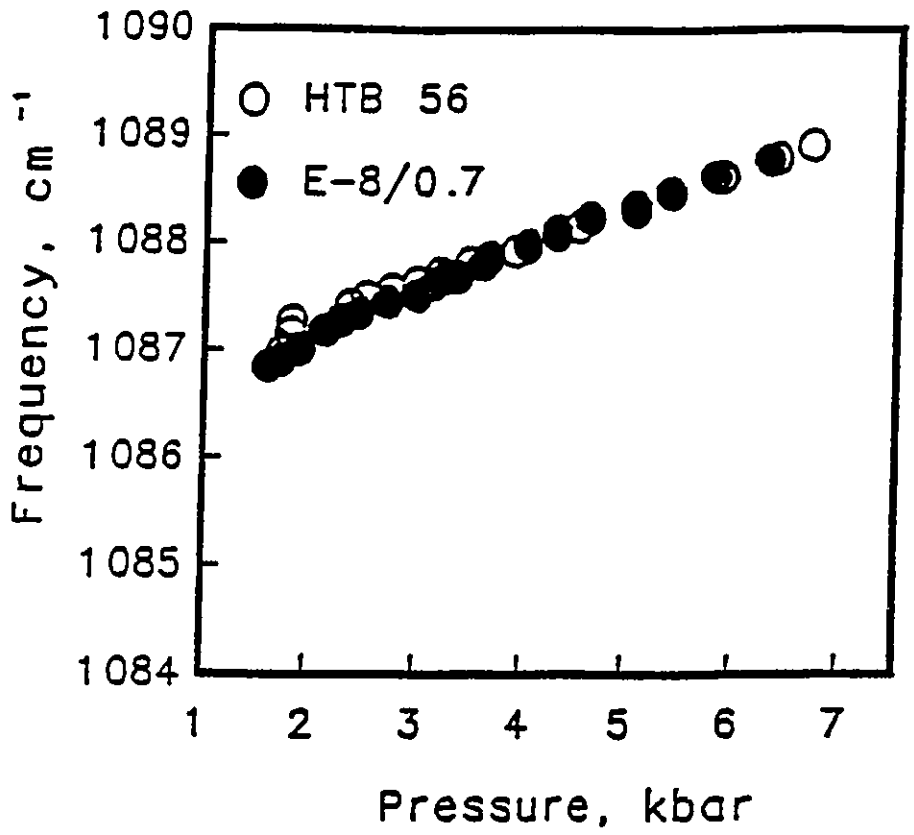

Figure 9: Pressure dependencies of the symmetric phosphate stretching frequencies of the HTB 56 and the E-8/0.7 cells. The position of the apex of the peak is plotted vs pressure, and gradually shifts to a higher frequency as pressure increases.

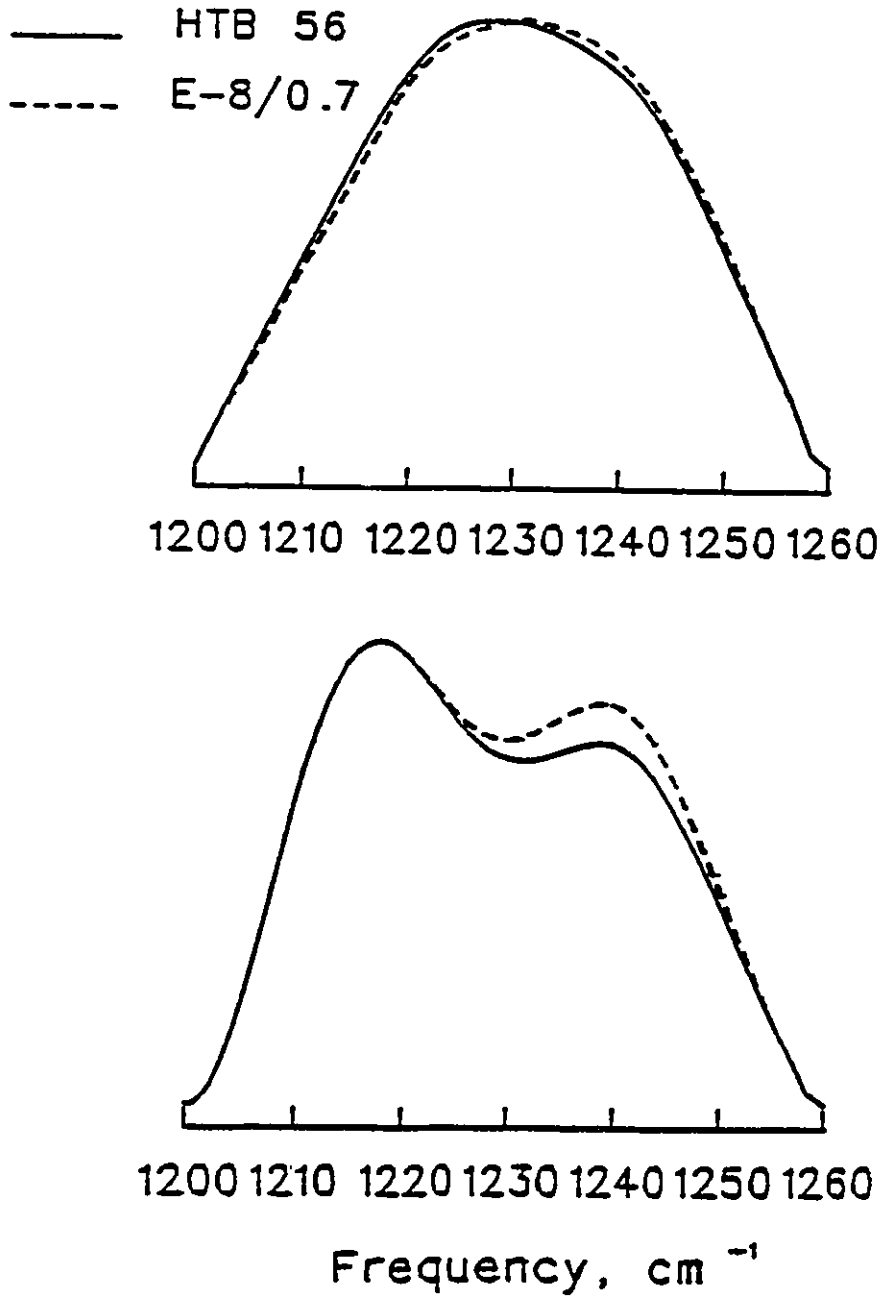

Figure 10: Original infrared spectra (at comparable pressure) in the $\nu_{as}PO_2^-$ region (top) of the HTB 56 and the E-8/0.7 cell lines, and the same spectra after the deconvolution with enhancement factor of 1.5 and band width 20 cm^{-1} (bottom).

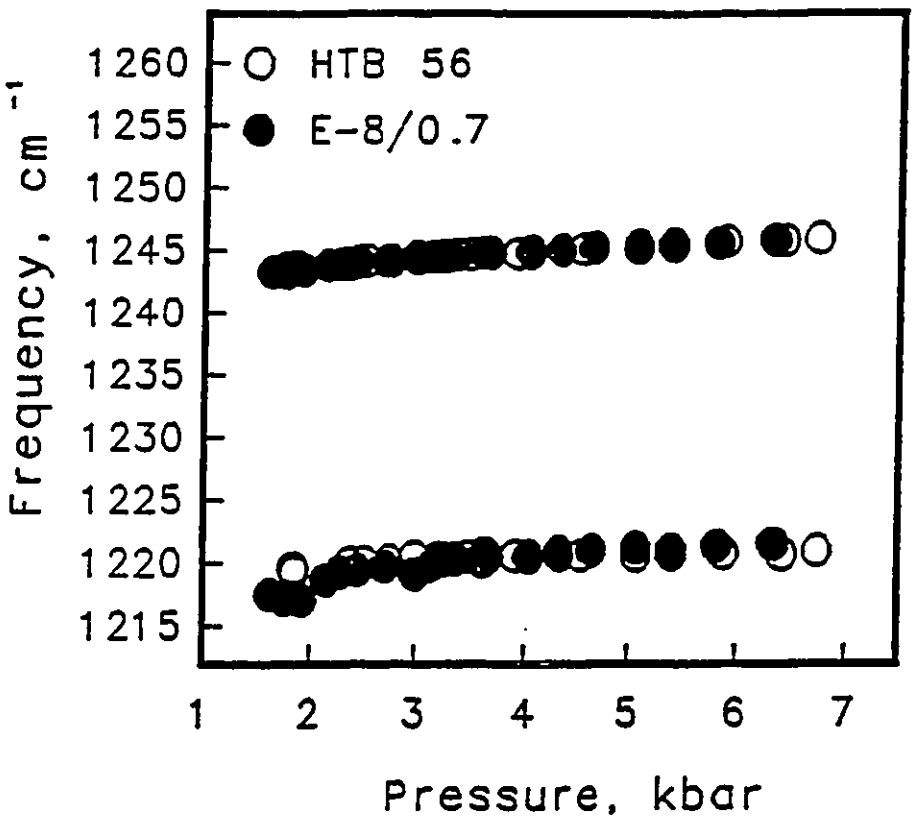

Figure 11: Pressure dependencies of the asymmetric phosphate stretching frequencies of the HTB 56 and E-8/0.7 cell lines. The frequencies of these bands were determined from the third order Fourier derivative spectra with a break point of 0.3 (Cameron 1987). There was minimal shift in these peaks as pressure increased.

Analysis of the C-O stretching band (figures 12 and 13) demonstrates that this band consists of three overlapping bands with peaks at ~1152 cm^{-1}, ~1167 cm^{-1} and 1175 cm^{-1}, respectively (figure 12). The first band displays the same intensity in both cell lines, whereas E-8/0.7 displays decreased intensity in the second and increased intensity in the third band, compared with HTB 56 cells. The component band ~1152 cm^{-1} has been observed in carbohydrate rich tissue and is superimposed on the glycogen band (Wong 1991[a]). The two other components of the C-O band, ~1167 cm^{-1} and 1175 cm^{-1}, are mainly from hydrogen and non-hydrogen bonded C-OH groups of three amino acids (serine, threonine and tyrosine) in cell proteins (Rigas 1990, Wong 1991[c]). It is also known that OH groups of serine, threonine and tyrosine that form C-O bonds observed here are sites of phosphorylation.

Analyses of the symmetric stretching CH_3 bending mode (figure 14) and the amide I band (figures 15) demonstrated that there is no difference detectable by PTIS in the structure of cellular proteins between HTB 56 and E-8/0.7 cells.

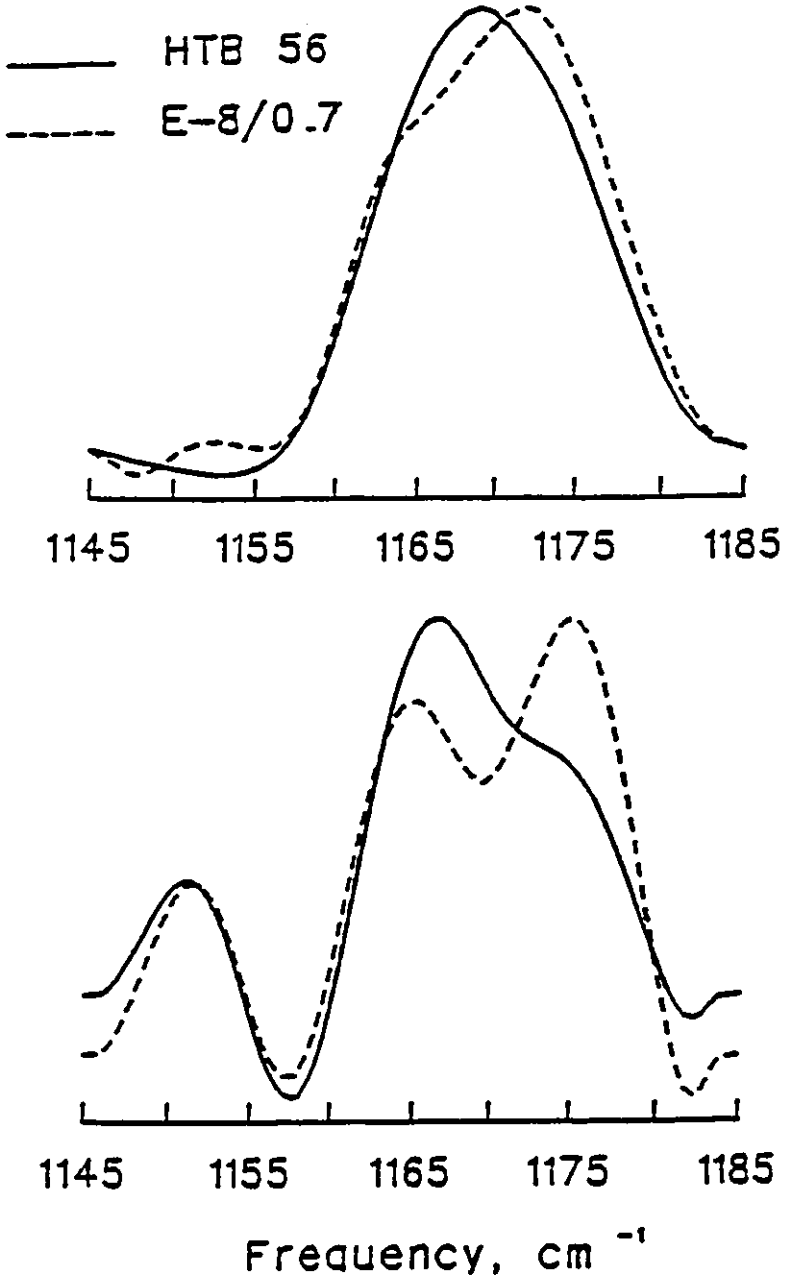

Figure 12: Original infrared spectra (at comparable pressure) of the HTB 56 and E-8/0.7 cell lines (top) and the same spectra after band narrowing at the bottom (band width 12 cm^{-1}, enhancement factor 1.45).

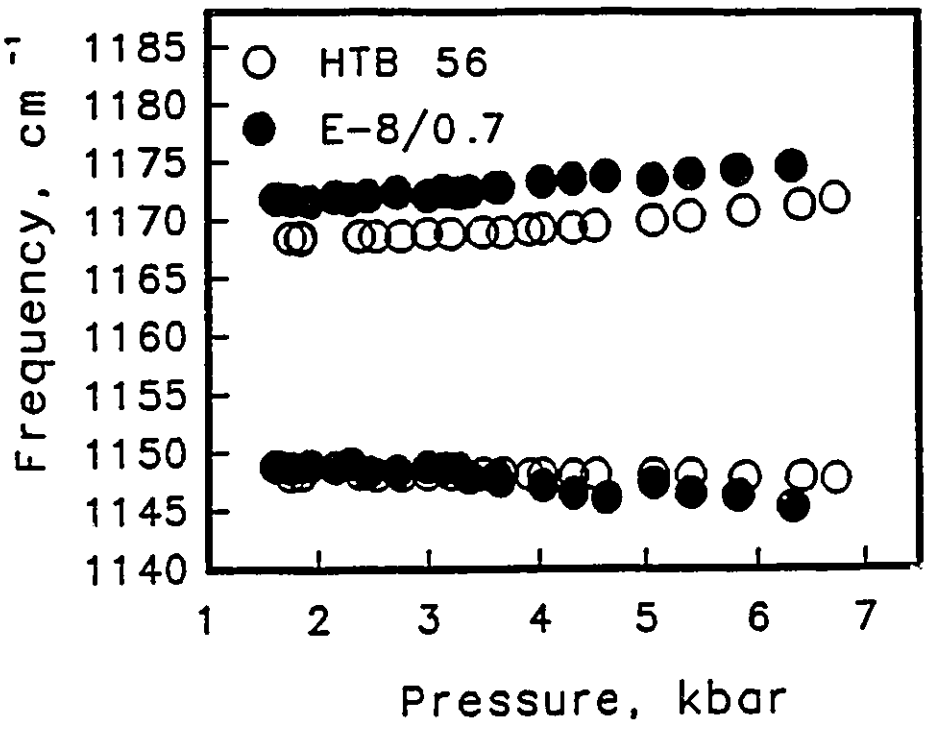

Figure 13: Pressure dependencies of the C-O band of cisplatin-sensitive and cisplatin-resistant cell lines. The frequencies were calculated from the third order Fourier derivative spectra using a breakpoint of 0.3. There were only minor peak shifts with increasing pressure. There was little difference between the HTB 56 and the E-8/0.7 cell lines.

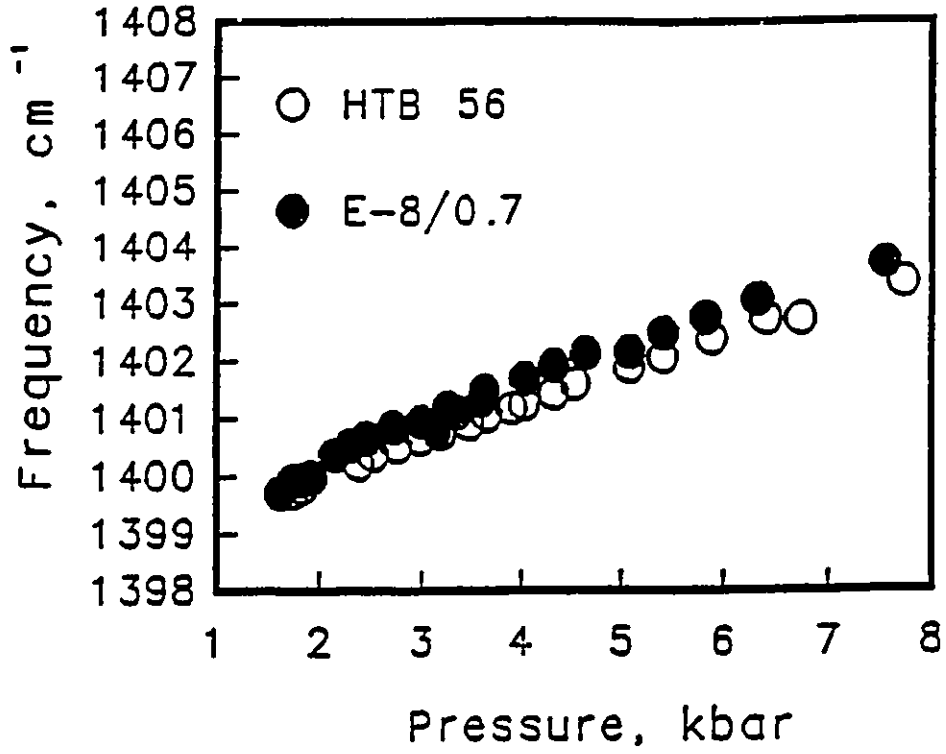

Figure 14: Pressure dependence of the frequency of the symmetric CH_3 bending mode of the HTB 56 and E-8/0.7 cells. The peaks shifted gradually with increased pressure.

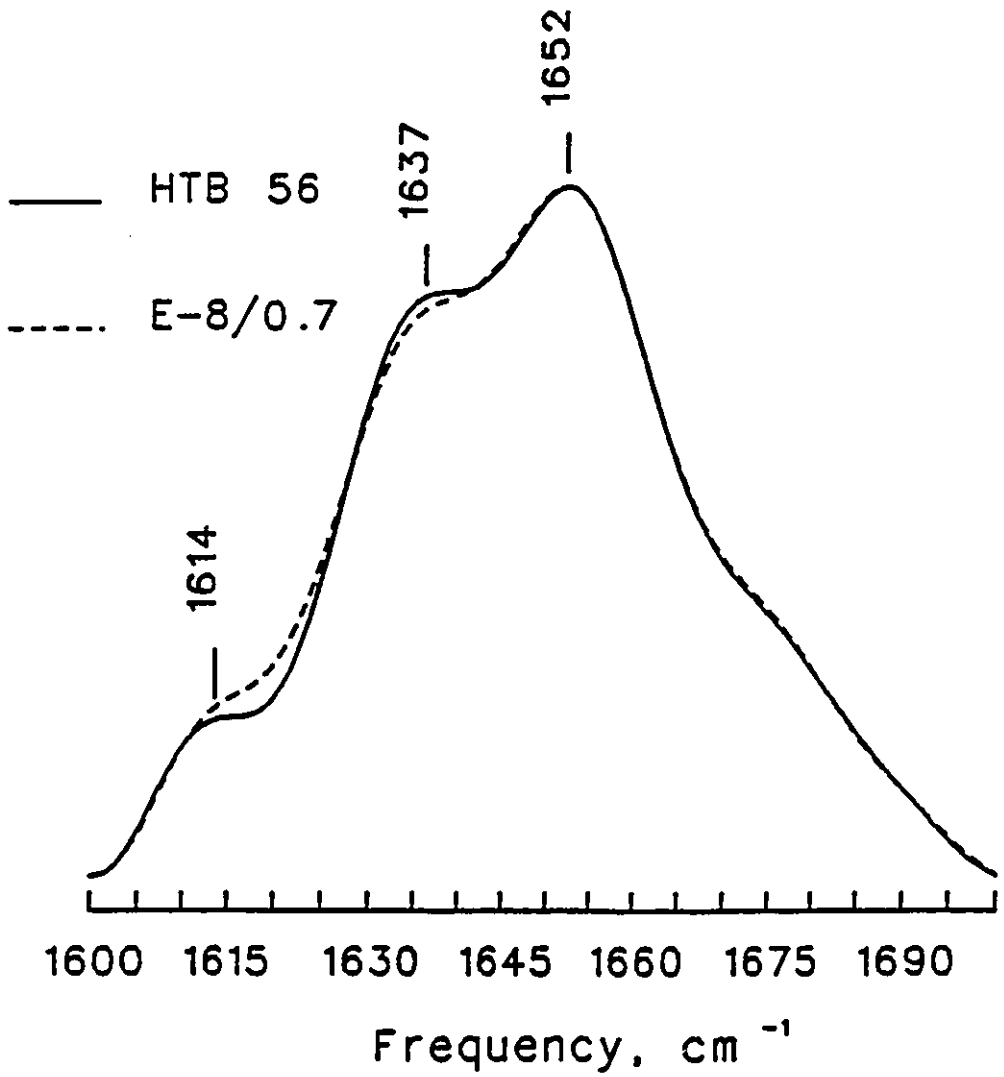

Figure 15: Infrared absorption band at atmospheric pressure of the amide I band of HTB 56 and E-8/0.7 cell lines after using Fourier self-deconvolution with a band width 20 cm^{-1} and a band narrowing factor of 1.5.

The amide I band represents mainly the stretching vibrations of C=O groups, weakly coupled with C-N stretching and in plane N-H bending vibrations (Susi 1969, Parker 1971). This band has been used by many investigators for determination of protein secondary structure (Wong 1989, Muga 1990, Ismail 1992). The amide I band is usually asymmetric and broad. It contains several overlapping bands, which can be seen using a deconvolution procedure that allows intrinsically overlapping bands to be resolved (Cameron 1987). The changes in the relative intensities of these peaks are used to monitor changes in the secondary structure of globular proteins. Deconvoluted spectra at normal pressure (figure 16) were obtained by Fourier self-deconvolution using a band width of 20 cm^{-1} and a resolution enhancement factor of 1.5. The peak around 1652 cm^{-1} originates from the α helix, suggesting that, in both cell lines, the protein secondary structure is mainly α helical. The peaks around 1637 cm^{-1} and ~1687 cm^{-1} represent the β sheet structure of proteins. The band around 1645 cm^{-1} was assigned to random coils, while the peak around 1615 cm^{-1} was assigned to intermolecular hydrogen bonds in proteins (Susi 1969).

Stacked contour plots of HTB 56 and E-8/0.7 cells (figure 16) and representative infrared spectra of a pair of these two cell lines in the CH region (figure 17) could not detect any structural differences between the two cell lines. However, when cells were exposed to high pressure (figures 18 and 19), some differences in structural and dynamic properties of methylene chains were observed. Studies of the pressure dependence of $\upsilon_s CH_2$ revealed that the disorder-order transition pressure (i.e. the pressure at which the peak begins to shift position) is ~1.0 kbar lower in E-8/0.7 cells than in HTB 56 cells (figure 18). From the same figure, it can be seen that this break point is ~3.02 kbar in E-8/0.7 cells, while it is 4.0 kbar in HTB 56 in this particular experiment. Over several experiments the mean value was 3.33 kbar (n=10) for E-8/0.7 cells, whereas it was 3.94 kbar (n=7) for HTB 56 cells ($p< 0.001$). The break point varied slightly from sample to sample due to experimental error, but it was always higher in HTB 56 cells than in E-8/0.7 cells. In $\upsilon_{as} CH_2$, similar phenomena were observed (figure 19), although because of noisy spectra under high pressure, the break point could not be determined in some cases. Because of the complexity of the asymmetric CH_2 stretching vibrations and

presence of Fermi resonance, this band is not very suitable for determination of disorder-order transition pressure (Wong 1992).

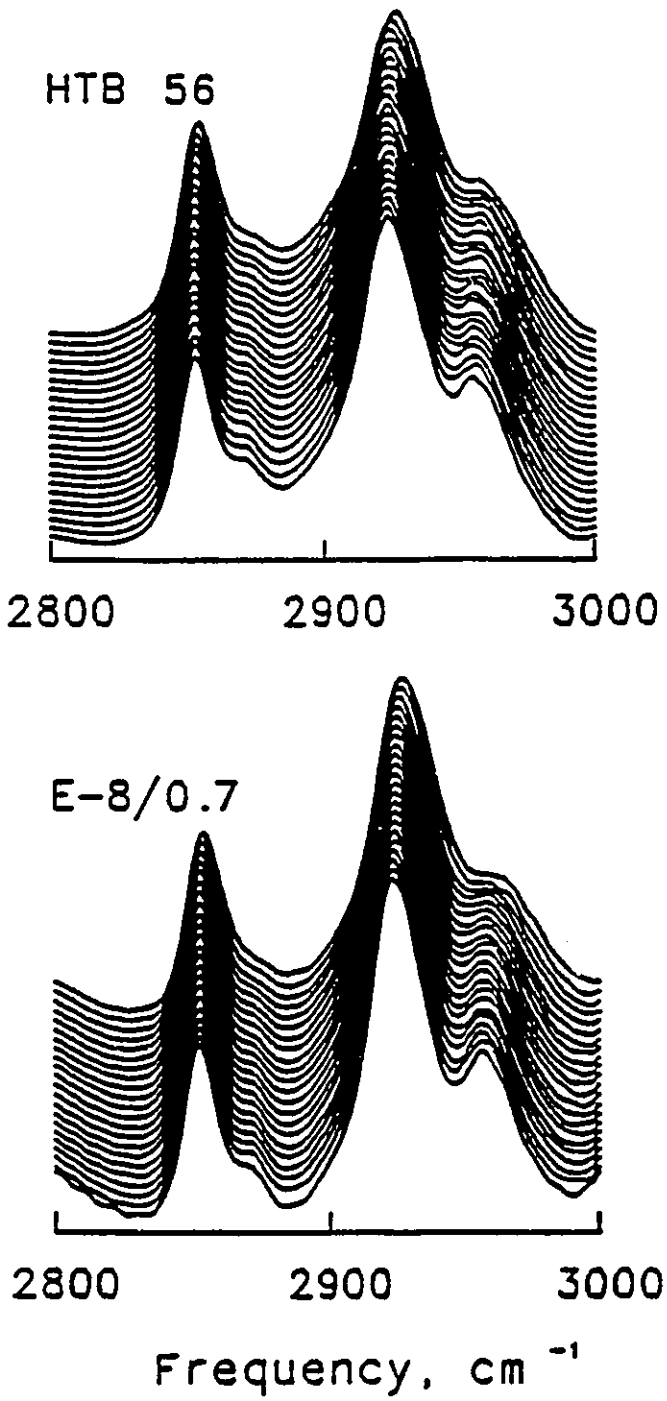

Figure 16: Stacked contour plots (absorbance vs frequency vs pressure [up to 10 kbar]) of the infrared spectra in the CH stretching mode region. The top contour plot represents the spectrum at the highest pressure tested (~10 kbar).

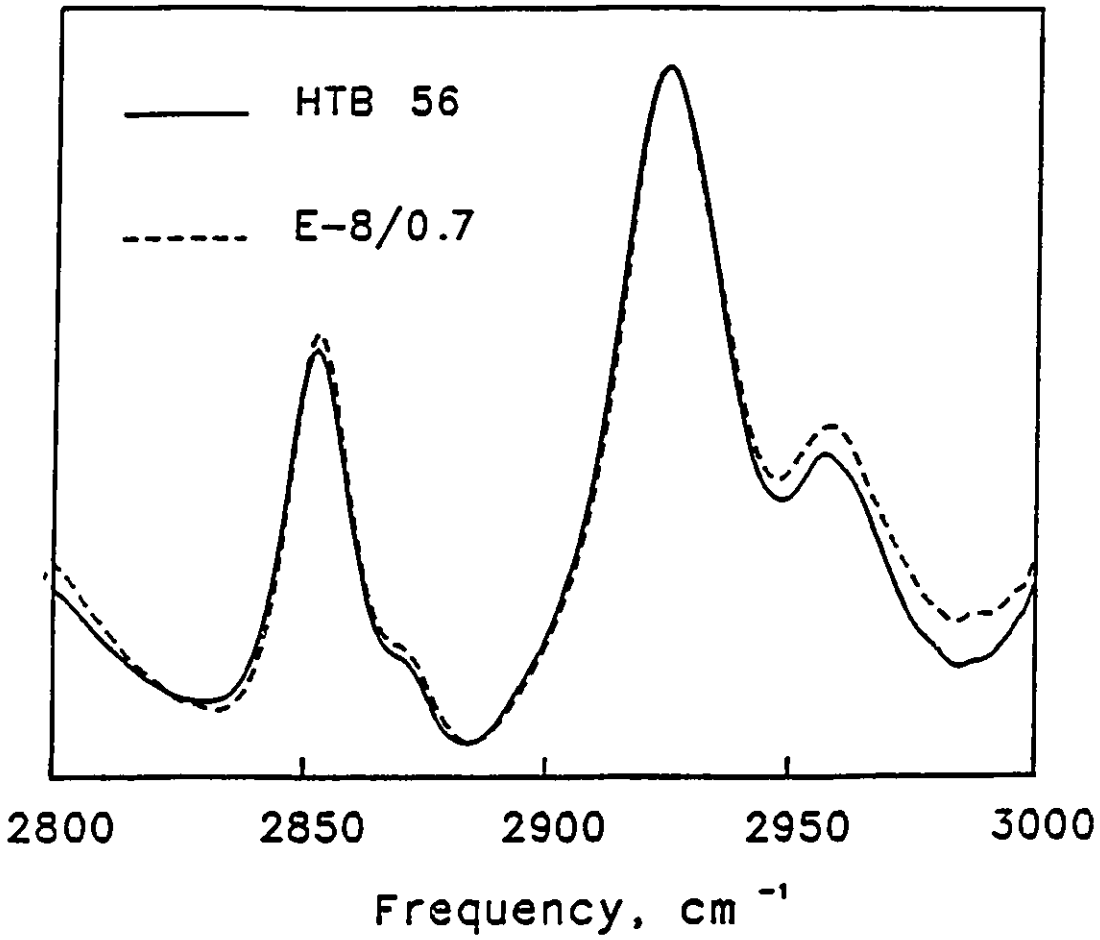

Figure 17: Representative pair of infrared absorption spectra of the HTB 56 and E-8/0.7 cell lines in the CH stretching region at comparable pressure.

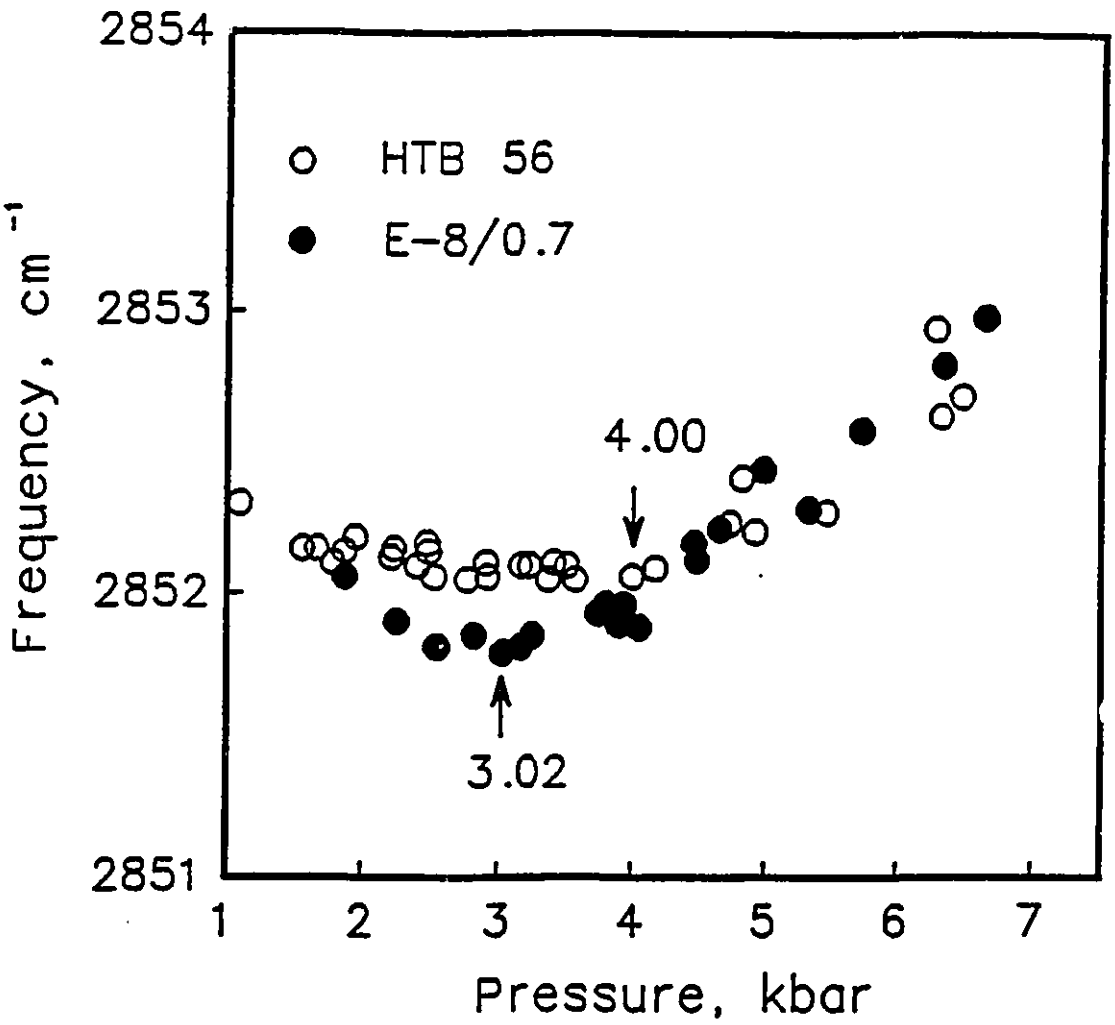

Figure 18: Pressure dependence of the symmetric CH_2 stretching frequencies of the HTB 56 and E-8/0.7 cells. The frequency positions were determined from the third order derivative spectra with a break point 0.3. The pressure at which the peak began to shift to a higher frequency represents the disorder-order transition pressure for the methylene chains. This transition pressure was lower for E-8/0.7 cells than for HTB 56 cells, indicating that the resistant E-8/0.7 cells have a more ordered (i.e., more rigid) membrane than do the HTB 56 cells.

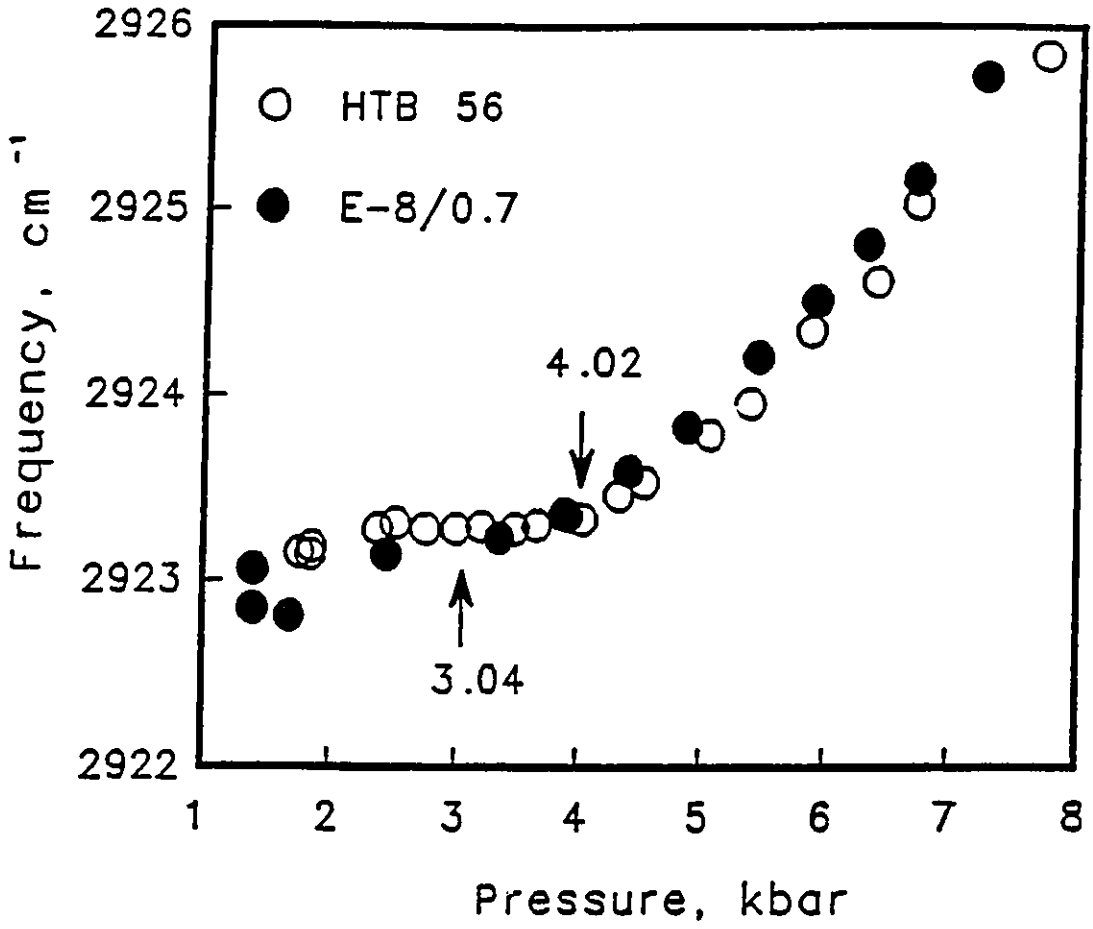

Figure 19: Pressure dependence of the frequencies of the CH_2 antisymmetric stretching mode of the HTB 56 and E-8/0.7 cells. The conclusions are the same as in figure 18.

3.5 Platinum cellular accumulation

The objective of this experiment was to determine whether the newly acquired resistance to cisplatin in our E-8/0.7 cell line was associated with decreased drug uptake. Basically, there are two major methods one may use to quantitate cellular platinum. One is the use of a gamma counter to measure radioactivity following administration of ^{195}Pt-labelled cisplatin (Andrews 1988), and the other is by analysis of cell lysate for platinum using flameless atomic absorption spectrophotometry (Timmer Boscha 1989, Mann 1990, Nishikawa 1990 etc.). Both methods measure elemental platinum in cells.

Cisplatin cellular accumulation was assayed by exposing cell monolayers in 60 mm tissue culture dishes to cisplatin (100 μM) for varying lengths of time (1, 5, 10, 15, 30 and 60 minutes). Cell exposure to cisplatin was conducted in IMDM media. IMDM media did not contain fetal calf serum for these drug accumulation experiments, because cisplatin can be irreversibly bound and inactivated by proteins. Only unbound cisplatin is considered to be therapeutically active (van der Vijgh 1986). Although cisplatin concentrations used in this

experiment were much higher than clinically achievable plasma concentrations, cells were still able to exclude trypan blue dye after 1 hour exposure, suggesting that membrane integrity was preserved. Aliquots of the sonicated cell suspension prepared as described in section 2.4.2 were assayed for platinum and protein. To correct for differences in cell numbers, proteins were assayed and results were expressed as pmol cisplatin/mg protein. Figure 20 illustrates platinum accumulation versus time.

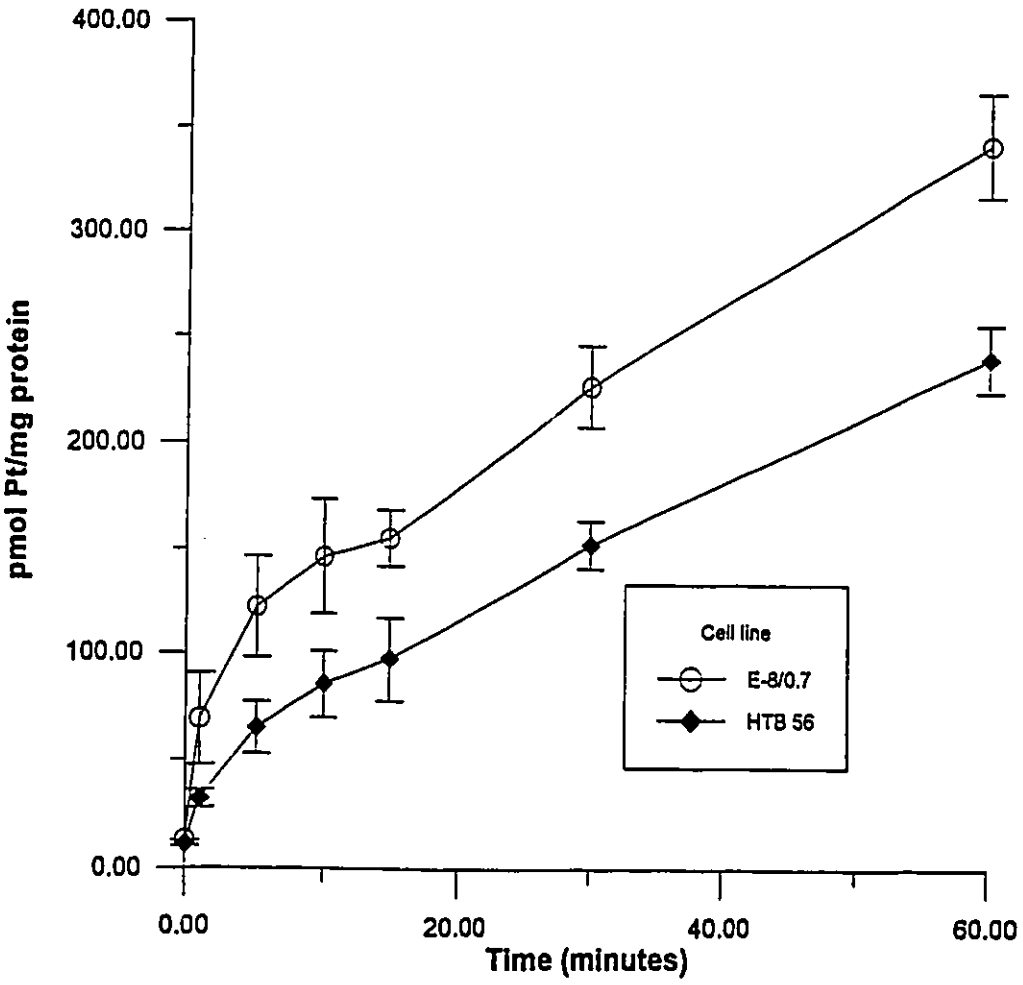

Figure 20: Platinum accumulation versus time after exposure to cisplatin 100 uM. Points represent mean of four experiments. The error bars represent standard error of the mean.

3.6 Lipid Analyses

The purpose of these experiments was to answer some questions related to decreased membrane fluidity in E-8/0.7 cells observed by pressure tuning infrared spectroscopy (see section 3.4). The modulators of membrane fluidity can be grouped into chemical modulators and effects of physical factors. The main chemical modulators are: i) Cholesterol level, expressed as the cholesterol to phospholipid molar ratio, ii) the degree of unsaturation of phospholipid acyl chains and the length of acyl chains, iii) the level of sphingomyelin and iv) membrane proteins (Shinitzky 1984). It should be noted that other phospholipids beside sphingomyelin can also affect fluidity. Sphingomyelin, phosphatidyl serine and phosphatidyl ethanolamine all decrease membrane fluidity, while phosphatidyl choline increases fluidity (Mann 1988).

Physical factors that affect membrane fluidity are temperature, pH, pressure, membrane potential and Ca^{++}. Effects of physical effectors can be seen almost immediately, in contrast to chemical modulators. Chemical modulators can be changed by passive exchange from the environment (medium, serum), or by membrane

biogenesis. Both processes need from several hours to several days to reach steady state.

In this study we assessed cell membrane content of major phospholipid classes and cholesterol.

Early plateau phase HTB 56 and E-8/0.7 cells were harvested by scraping them into sterile isotonic saline. Cells were pelleted, covered with a few ml of 0.9% NaCl and stored at -80°C until analyzed. The cell lipid extracts were separated into major phospholipid classes by one dimensional thin layer chromatography (section 2.7.2.2). Although some authors prefer two dimensional thin layer chromatography because of better separation, figures 21 and 22 show that we had very good separation of major phospholipid classes, using one dimensional thin layer chromatography. Bands were identified by I_2 vapour. Identified bands were analyzed for phosphate by a modified Rouser procedure. Three pairs of HTB 56 and E-8/0.7 were simultaneously analyzed. Overall, phosphorus measurements were performed 9 times in HTB 56 cells and 10 times in E-8/0.7 cells. Since standard deviations were relatively large, and since the data did not conform to a normal distribution, data were analyzed by the non-parametric Mann-Whitney statistical test.

Table 3 reveals that phosphatidyl choline and phosphatidyl ethanolamine were the predominant phospholipids in both cell lines, as observed in other cell lines and tissues (Mann 1988, Calorini 1989, Ruiz-Gutirrez 1992). The only significant difference ($p < 0.03$) in E-8/0.7 cells from the corresponding value in the parent cell line was in the concentration of sphingomyelin (~21.7% vs ~14.02% [table 3]). Since both of our cell lines were cultivated, harvested and analyzed together, differences in sphingomyelin content cannot be explained on the basis of different medium or experimental conditions. Although phosphatidyl choline and especially phosphatidyl serine values look quite different, their median values analyzed by non-parametric tests showed that the differences are not significant. Surprisingly, both cell lines had a relatively high concentration of sphingomyelin compared to other malignant cell lines, even higher than in glioma cell lines (Calorini 1987, Mann 1988, Murphy 1993).

Although sphingomyelin, like phosphatidyl choline is a phosphorylcholine they have quite different physicochemical properties. Phosphatidyl choline is the most fluidizing membrane phospholipid, whereas

sphingomyelin is the most rigidifying phospholipid of the lipid bilayer (Shinitzky 1984).

TABLE 3 PHOSPHOLIPID COMPOSITION OF HTB 56 AND E-8/0.7 CELLS*

PL CLASS	HTB 56	E-8/0.7
PC	56.05±3.0	51.02±1.5
PE	21.43±2.5	23.22±0.9
SPH	14.02±1.4	21.71±0.8**
PS	5.43±1.4	1.77±0.7
PC/PE	2.49±0.29	2.25±0.17
PC/SPH	4.45±0.55	2.44±0.2**

* Reported as mol % of total phospholipid content. Values are means ± SE of 9-10 measurement of 3 separate pairs of both cell lines.

** Significant difference ($p<0.03$) from the corresponding value in the parent cell line.

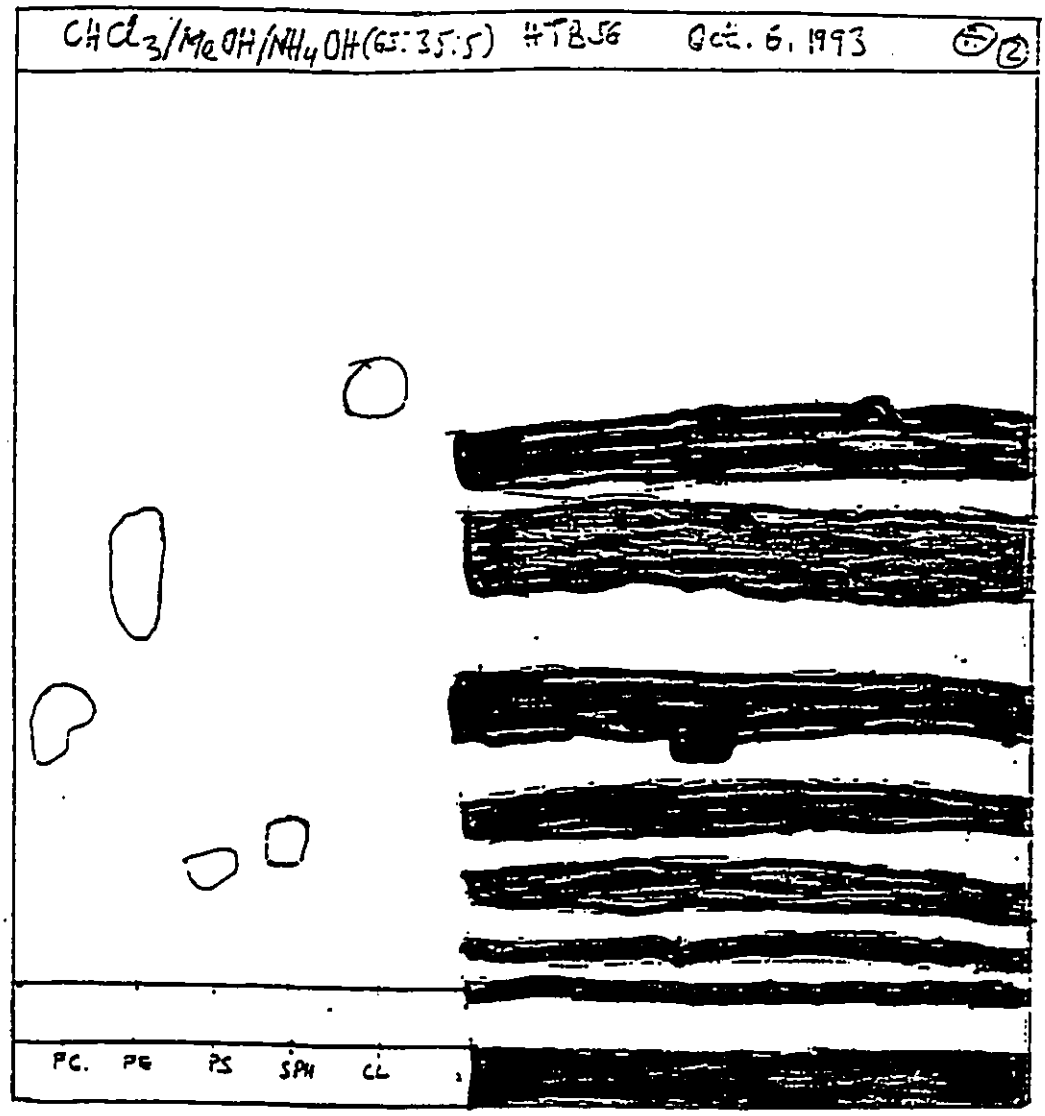

Figure 21: Scraped bands of major phospholipid classes of HTB 56 cells after thin layer chromatography.

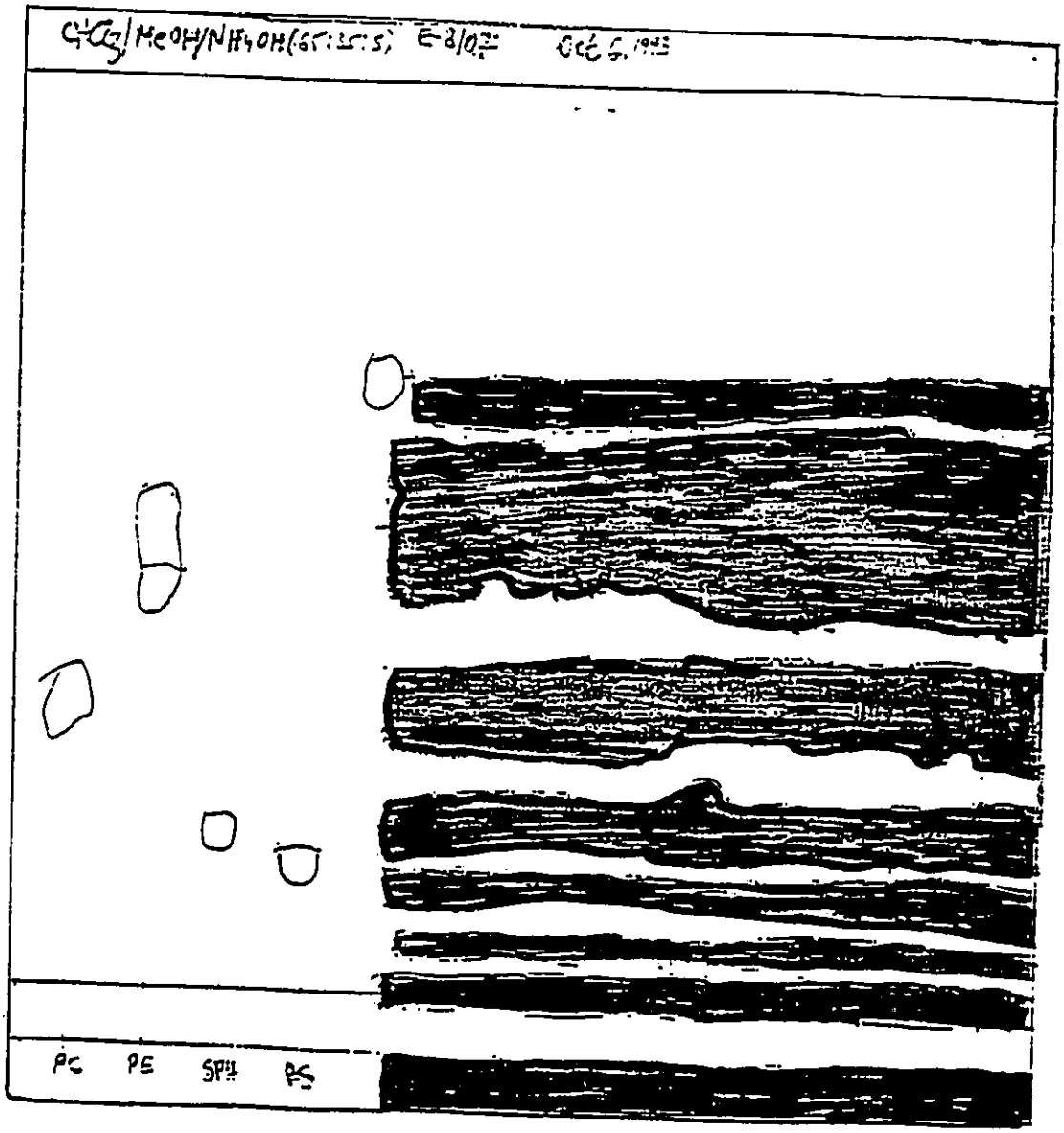

Figure 22: Scraped bands of major phospholipid classes of E-8/0.7 cells after thin layer chromatography.

3.6.2 Cholesterol analysis

Total cholesterol content of HTB 56 and E-8/0.7 cells in plateau phase was analyzed by the method originally described by Zlatkis. Although some authors prefer enzymatic methods because of higher sensitivity, we found that the colorimetric method used in this study was highly reproducible, and the standard curves passed through the origin. We found that the total cholesterol levels in both cell lines were essentially the same (table 4). However, total phospholipid levels in the E-8/0.7 cells were ~12% lower than in the HTB 56 cells. This decrease resulted in a slightly higher cholesterol to phospholipid molar ratio in the resistant variant than in HTB 56 cells, potentially contributing to the lower fluidity of cell membranes in the E-8/0.7 cells. Although the difference in the ratio was small, it was statistically significant ($p<0.01$).

Table 4 Cholesterol and phosphorous content in the HTB 56 and E-8/0.7 cells

SPECIES	HTB 56	E-8/0.7
µg Choles/mg protein	29.48±3.3	29.44±0.89
µg Total P/mg protein	7.38±0.9	6.48±0.25
Total chol/PL molar ratio	0.33±0.01	0.38±0.01*

Values are means ± SD of 9 measurement

* Significant difference ($p < 0.01$) from the corresponding value in the parent cell line

4.0 DISCUSSION

4.1 Establishment of cisplatin resistant cell line

There is no widespread agreement which model system is the best for the study of drug resistance because the environment of the cells in vitro is different from that in vivo and may alter their chemosensitivity (Ludwig 1984). Most investigators have used cell lines that have acquired drug (cisplatin) resistance (Kikuchi 1986, Teicher 1987, Fujiwara 1990 etc.), while many fewer utilized in vivo tumour lines (Teicher 1990, Andrews 1990, O'Dwyer 1994).

In our dose response studies of commercially available human NSCLC cell lines, we found that the HTB 56 adenocarcinoma cell line was relatively sensitive to cisplatin (figure 2). Consequently it was very suitable for the study of development of cisplatin resistance. We wished to produce a cell line with a low or moderate degree of resistance, since cisplatin clinical resistance is probably low level as opposed to high level (Oldenburg 1994).

Our newly established cisplatin resistant subline, E-8/0.7, offers an excellent model system for studies of cisplatin resistance because a) it is a rapidly growing cell line; b) resistance is stable; c) a higher degree of resistance is easily achievable; d) cells grow attached to the bottom of the flask; e) the E-8/0.7 cells show high viability after cryopreservation (sections 2.2 and table 2); and f) studies underway indicate involvment of a number of mechanisms of resistance to cisplatin (in addition to increased drug uptake) that can be studied.

4.2 PTIS analysis of HTB 56 and E-8/0.7 cells

Infrared studies of cells and tissues have been hampered by a strong water band in the region of interest, by problems in sample preparation and by suboptimal spectra acquisition. However, recent methodological and technological improvements, as well as application of high pressure, have made pressure tuning infrared spectroscopy an increasingly powerful tool in the study of cellular structure. It should be emphasized that this technique investigates structural

and dynamic properties of cell macromolecules in intact (unprocessed) cells and tissues. This is important, since structural properties of isolated cell macromolecules are no longer the same as they are in intact cells or tissues. Most of the infrared studies of malignant cells have focused on the potential applicability of this technique as a diagnostic tool in detection of malignancy (Benedetti 1990, Wong 1991[c]). There are no data in the literature regarding use of PTIS to study drug (cisplatin) sensitive and resistant cells. Because of the very high similarity of cisplatin sensitive cells to their resistant variants, high quality of spectra and advanced instrumentation are required to detect differences.

Compared to HTB 56, E-8/0.7 cells showed major changes in symmetric and asymmetric stretching vibrations of CH_2 groups of membrane lipids. The shifted break point in E-8/0.7 cells (figure 18), indicates a decrease in the pressure that is required to completely dampen the reorientational mobility of methylene chains. Approximately -0.6 kbar lower pressure was needed to produce a high degree of order of methylene chains in E-8/0.7 cells than in HTB 56 cells, indicating reduced membrane fluidity in E-8/0.7 cells (Wong 1988, Wong

1992). Our initial PTIS studies of the CH region were carried out in samples hydrated with deuterated water (to reduce the background noise associated with regular water). However, an unexpectedly high quality of spectra (ie, high signal to noise ratio) in regular water allowed us to study the break point in the CH_2 region even in samples hydrated with isotonic saline. This substantially simplified sample preparation for study of the CH region (2800-3000 cm^{-1}).

We also observed similar PTIS membrane fluidity findings in two other malignancies resistant to cisplatin due to reduced drug uptake (the C13*, human ovarian cancer cell line and the EMT-6/DDP, subcutaneously grown murine mammary tumour). Our results raise the question whether PTIS can be used to predict tumour response to cisplatin treatment.

We also found decreased intensity of hydrogen bonded C-O groups in E-8/0.7 cells (figure 12), which could be due to increased phosphorylation (Rigas 1990). In addition, increased phosphorylation of nuclear phosphoproteins has been reported in lung cancer cell lines resistant to cisplatin (Nishio 1992). However, it should be emphasized that the observed changes in the C-O band was not seen in all analyzed samples and that

the intensities of these peaks varied within the same sample in repeated experiments.

4.3 Platinum accumulation

Experiments carried out to determine cisplatin accumulation in HTB 56 and E-8/0.7 cells revealed about a 30 % decrease in platinum uptake in cisplatin-resistant cells (section 3.5 and figure 20). This finding strongly supports our hypothesis that diminished drug uptake plays an important role as an initial mechanism of cisplatin resistance. However, platinum accumulation does not correlate very well with the actual degree of cisplatin resistance, especially at high levels of resistance (Mann 1990, Fujiwara 1990). We have also noted that increasing resistance from the E-8/0.5 subline to the E-8/0.7 subline was not accompanied by a proportional decrease in drug accumulation, suggesting that reduced drug uptake is not the only mechanism of cisplatin resistance in E-8/0.7 cells. Cisplatin accumulation appears to be linear between 10 and 60 minutes in both cell lines. Correlation coefficients (r) and r^2 values were 0.9962 and 0.9932,

respectively, for HTB 56 cells, and were 0.9988 and 0.9975, respectively, for E-8/0.7 cells. Cisplatin uptake from 0 to 10 minutes was non-linear in both cell lines (figure 20). There are a number of possible explanations for this. For example, this might have occured due to initial rapid influx, with subsequent activation of an efflux mechanism that partially overcame the effect of influx. This uptake pattern might also have resulted from a time-dependent hydrolysis of native cisplatin into various species with differing membrane transport and intracellular binding characteristics. In addition, temperature fluctuations during the early part of incubation may have resulted in nonlinearity of drug uptake.

It should be noted that our cisplatin uptake analyses provided no information regarding cisplatin's location within the cell (nuclear vs cytoplasmatic vs plasma membrane). Moreover, cisplatin's chemical form (native vs aquated species, etc.) cannot be determined by our AA methodology. In spite of these disadvantages, this method is widely accepted in cisplatin pharmacology studies, and cellular platinum content correlates very well with cisplatin cytotoxicity. Modulation of cisplatin accumulation by hyperthermia (Kimura 1993) or

some drugs, such as amphotericin B (Morikage 1991) can decrease or even reverse resistance to cisplatin. In preclinical studies, many investigators have reported positive correlations between cellular platinum accumulation and cisplatin cytotoxicity in different tumour types (Richon 1987, Andrews 1988, Bungo 1990 etc.), and platinum concentrations in human autopsy tumour samples were higher in patients who had responded initially to cisplatin treatment than in patients who had failed to respond (Stewart 1988).

Decreased cisplatin accumulation appears to be due to decreased drug uptake rather than increased drug efflux (Andrews 1988). However, the way(s) whereby cisplatin enters cells remains poorly understood.

4.4 Lipid analyses

4.4.1 Phospholipid analyses

The search for the cause of increased rigidity of cell membranes in cisplatin-resistant cells led to an analysis of cell lipids in HTB 56 and E-8/0.7 cell

lines. Quantitative analyses of phospholipids revealed a significantly higher level of sphingomyelin in E-8/0.7 cells compared to HTB 56 cells (table 3). High sphingomyelin content is generally regarded as a feature associated with increased membrane rigidity (van Blitterswijk 1987).

Although we do not know the precise cellular location of sphingomyelin from our analysis of cell homogenates, sphingomyelin is preferentially located in plasma membranes (Rana 1993, Yeagle 1989). In addition, it is known that the plasma membranes are the major cellular site of cholesterol accumulation (De Gier 1968, May 1986), and that cholesterol has a higher affinity for sphingomyelin than for other classes of phospholipids (Boggs 1987). It has been shown that the activity of 5' nucleotidase (which is located in the outer leaflet of the plasma membrane and which serves as a plasma membrane marker) is dependent on sphingomyelin (Sandermann, Jr 1978). Moreover, even after treatment with an excess of detergent, 5' nucleotidase will retain sphingomyelin. It has also been reported that in human platelets, intracellular membranes are substantially depleted in sphingomyelin, while surface membranes are enriched in this phospholipid (Lagarde 1981, Fauvel

1986, Rana 1993). Sphingomyelin plays a major role in increasing rigidity of membrane lipid bilayers, in decreasing membrane permeability, and in modulation of activity of membrane-based enzymes such as phospholipase C (Wood 1986, Daveloose 1993).

Sphingomyelin probably contributed to the increased membrane rigidity in our E-8/0.7 cell line. The molar ratio of sphingomyelin to phosphatidyl choline was significantly higher in the E-8/0.7 cell line than in the HTB 56 cell line ($p<0.03$) (table 3). This ratio is an important factor in cell membrane fluidity (Shinitzky 1984, Daveloose 1993).

We do not know whether the reduced cisplatin uptake of E-8/0.7 cells is due to the cell line's increased membrane rigidity and increased sphingomyelin content, or whether the association is coincidental. However, in related PTIS studies, we also found that membrane fluidity was decreased in the cisplatin-resistant C13* human ovarian cancer cell line and in the EMT-6/DDP murine mammary tumour (both of which have reduced cisplatin uptake) compared to their cisplatin sensitive parents (Popovic 1992, Popovic 1993[a&b]). On the other hand, the cisplatin-resistant U373MG/DDP human glioma cell line, which has normal cisplatin uptake, had

membrane fluidity that was comparable to the cisplatin-sensitive parent cell line (Stewart 1993), as did a cyclophosphamide resistant variant of the EMT-6 tumour (Popovic 1993[a]). Other members of our group have also found in PTIS studies that cisplatin may be capable of diffusing across fluid phosphatidyl choline model membranes, while it is not capable of diffusing across more rigid phosphatidyl serine and phosphatidyl ethanolamine model membranes (Taylor 1992, Taylor 1993).

4.4.2 Cholesterol analysis

Cholesterol is an essential component of the membranes of all animal cells, and is essential for cell growth. In most cells, cholesterol is present mainly in the plasma membrane. Much less is presents in the endoplasmatic reticulum, mitochondrial and lysosomal membranes. The cholesterol molecule has a nucleus of four fused rings common to all sterols. Most of the molecule is hydrophobic, while the hydroxyl group at C-3 is polar and enables cholesterol to interact with other lipids such as fatty acids and phospholipids. It should be emphasized that pure cholesterol at body temperature

is in a solid state (since its melting point is 150°C). In the plasma and cells, cholesterol crystallization is prevented by its interaction with phospholipids. The physical properties of an artificial phospholipid bilayer without cholesterol are such that it cannot function efficiently as a biological membrane. In liposomes, cholesterol increases the order of methylene chains in the liquid crystalline phase, while decreasing the order of methylene chains in the gel phase (Cheng 1986). The effect of this is to stabilize the bilayer over a wide range of temperatures in an intermediate fluid condition.

It has been suggested that cholesterol is the most important membrane rigidifying factor under physiological conditions. The principal determinant of the bulk lipid fluidity in cell membranes is the mole ratio of cholesterol to phospholipids (van Blitterswijk 1987, Shinitzky 1984). A higher value of that ratio corresponds to higher membrane rigidity and vice versa.

Cholesterol can effectively reduce membrane permeability and alter the transport rate of a solute across a lipid bilayer (Marsh 1973). The influence of cell membrane lipid constituents on permeability to some drugs (e.g. cisplatin) is not yet clearly defined. It

has been demonstrated that cholesterol decreases permeability of non-electrolytes in liposomes to a degree proportional to the concentration of cholesterol (De Gier 1968). There is evidence that in natural membranes, cholesterol is found on the opposite side of the bilayer from phosphatidyl ethanolamine and phosphatidyl serine, but on the same side as sphingomyelin and phosphatidyl choline (Boggs 1987). Cholesterol has a higher affinity for sphingomyelin than for other phospholipids, and both compounds have a strong rigidifying effect on the cell membrane. Assuming that cisplatin enters cells by passive diffusion, one might presume that packing and structural order of membrane lipids should affect that diffusion process.

Membrane cholesterol may modulate plasma membrane protein activity, probably by a direct cholesterol-protein interaction (Yeagle 1988, Warren 1975). It has been noted in many tissues that activity of Na+,K+-ATPase was inhibited by high membrane cholesterol levels (Yeagle 1989). It is well known that Na+,K+-ATPase is the primary generator of the membrane potential. Low levels of cholesterol in plasma membranes stimulate this enzyme (Yeagle 1988). An elevation of plasma membrane potential in an ovarian cancer cell line resistant to

cisplatin due to decreased cisplatin intake has been reported (Andrews 1992).

It seems that the lower cholesterol/phospholipid molar ratio in the E-8/0.7 cell line compared to the HTB 56 cell line may be due to decreased total phospholipid content in E-8/0.7 cells compared to HTB 56 cells (table 4). The lower levels of phospholipids in the resistant subline could be due to decreased phospholipid biosynthesis, accelerated phospholipid breakdown, or both. Our findings agree with the observation that vincristine uptake in three leukaemic cell lines was inversely proportional to the cholesterol to phospholipid molar ratio. Moreover, the same study showed that drug uptake was modulated by cholesterol depletion and loading (Pallares-Trujillo 1993). It is very possible that one of the factors which decreased cisplatin uptake in our E-8/0.7 cells was the altered cholesterol/phospholipid molar ratio. Cholesterol is able to decrease the surface area occupied by phospholipids in monolayers (Bittman 1984). Presumably, cells with the same overall size, but with a higher cholesterol content or a higher cholesterol to phospholipid molar ratio, might have a smaller available surface for drug uptake.

Our findings indicate that changes in the cholesterol to phospholipid molar ratio and sphingomyelin content are factors that probably contributed significantly to the alterations in the physico-chemical properties of cell membranes in the E-8/0.7 cell line. However, it is possible that other factors such as phospholipid acyl chains also contributed to the increased membrane rigidity of E-8/0.7 cells.

4.0 CONCLUSIONS

Many studies of human cell lines have shown cisplatin resistance to be multifactorial. There are only a few reports in the literature regarding early onset mechanisms of cisplatin resistance in NSCLC cell lines.

Our results indicate that the newly developed cisplatin-resistant human adenocarcinoma cell line (E-8/0.7) has reduced cisplatin uptake, increased membrane rigidity, increased sphingomyelin content and an increased cholesterol to phospholipid molar ratio compared to the cisplatin-sensitive HTB 56 parent cell line. These studies suggest that altered membrane lipid composition in the resistant cell line results in increased membrane rigidity, which either decreases cisplatin passive diffusion into cells or else alters the activity of active transport processes in the cell membrane. This reduced cisplatin uptake probably accounts for some (but not all) of the cisplatin resistance seen in the E-8/0.7 cell line.

4.1 Areas for future research

In this study, we examined platinum content in cell homogenates. Determination of platinum concentration in cell organelles could also be valuable, especially since some recent reports have challenged the widely accepted opinion that cisplatin cytotoxicity correlates with platinum concentrations in DNA. Other cellular targets may also be very important.

We found that cisplatin-resistant E-8/0.7 cells had increased membrane rigidity, increased sphingomyelin content and increased cholesterol/phospholipid molar ratio. Other factors that can alter membrane fluidity, such as membrane proteins and particulary, length and number of unsaturated bonds in phospholipid acyl chains, should also be investigated.

Once the nature of the cisplatin resistant subline is better defined, specific strategies can be devised in an attempt to augment platinum accumulation and cisplatin cytotoxicity.

In future research, we will also determine whether a shifted disorder-order transition pressure in cisplatin-resistant cells is found in other cell lines and tumours with decreased drug uptake. If so, PTIS

could be employed clinically to attempt to predict patient response to cisplatin therapy.

REFERENCES

Alpert NL, Keiser WE, and Szymanski HA (1973). IR: theory and practice of infrared spectroscopy. "Plenum/Rosetta edition" pp 77-182.

Andrews PA, Velury S, Mann SC, and Howell SB (1988). cis-Diamminedichloroplatinum(II) accumulation in sensitive and resistant human ovarian carcinoma cells. Cancer Res. 48: 68-73.

Andrews PA and Howell SB (1990). Cellular pharmacology of cisplatin: perspectives on mechanisms of acquired resistance. Cancer Cells 2: 35-42.

Andrews PA and Albright KD (1992). Mitochondrial defects in cis-diamminedichloroplatinum (II)-resistant human ovarian carcinoma cells. Cancer Res. 52: 1895-1901.

Banwell CN (1972). Fundamentals of Molecular Spectroscopy, 2nd edition, McGraw-Hill Book Company (UK), pp 65-119.

Behrens BC, Hamilton TC, Masuda H, Grotzinger KR, Whang-Peng J, Louie KG, Knutsen T, McKoy WM, Young RC and Ozols RF (1987). Characterization of a cis-Diamminedichloroplatinum(II)-resistant human ovarian cancer cell line and its use in evaluation of platinum analogues. Cancer Res. 47: 414-418.

Benedetti E, Teodori L, Trinca ML, Vergamini P, Salvati F, Mauro F and Spremolla G (1990). A new approach to the study of human solid tumor cells by means of FT-IR microspectroscopy. Appl. Spectrosc. 44: 1276-1280.

Bevers EM, Tilly RHJ, Senden MG, Comfurius P and Zwaal RFA (1989). Exposure of endogenous phosphatidylserine at the outer surface of stimulated platelets is reversed by restoration of aminophospholipid translocase activity. Biochemistry 28: 2382-2387.

Bittman R, Clejan S, Lunz-Katz S and Phillips MC (1984). Influence of cholesterol on bilayers of ester and ether linked phospholipids. Permeability and ^{13}C-nuclear magnetic resonance measurements. Biochim. Biophys. Acta 772: 117-126.

Bligh EG and Dyer WJ (1959). Canadian J. Biochem. Phys. 37: 911-917.

Boggs JM (1987). Lipid intermolecular hydrogen bonding: influence on structural organization and membrane function. Biochim. Biophys. Acta 906: 353-404.

Bradford MM (1976). A rapid and sensitive method for the quantitation of microgram quantities of protein utilizing the principle of protein-dye binding. Analyt. Biochem. 72: 248-254

Bungo M, Fujiwara Y, Kasahara K, Nakagawa K, Ohe Y, Sasaki Y, Irino S and Saijo N (1990). Decreased accumulation as a mechanism of resistance to cis-Diamminedichloro platinum(II) in human non-small cell lung cancer cell lines: relation to DNA damage and repair. Cancer Res. 50: 2549-2553.

Calorini L, Fallani D, Tombaccini G, Mugnai G and Ruggieri S (1987). Lipid composition of cultured B16 melanoma cell variants with different lung-colonizing potential. Lipids 22: 651-656.

Calorini L, Fallani A, Tombaccini D, Barletta E, Mugnai G, Di Renzo MF, Comoglio PM and Ruggeri S (1989). Lipid characteristics of RSV-transformed balb/c 3T3 cell lines with different spontaneous metastatic potentials. Lipids 24: 685-690.

Cameron DG and Moffatt DJ (1987). A generalized approach to derivative spectroscopy. Appl. Spectrosc. 41: 539-544.

Canadian Cancer Statistics (1993), National Cancer Institute of Canada.

Casal HL and Mantsch HH (1984). Polymorphic phase behaviour of phospholipid membranes studied by infrared spectroscopy. Biochim. Biophys. Acta 779: 381-401.

Cheng KH, Lepock JR, Hui SW and Yeagle PL (1986). The role of cholesterol in the activity of reconstituted Ca-ATPase vesicles containing unsaturated phosphatidyl ethanolamine. J. Biol. Chem. 261: 5081-5087.

Cross AD (1964). An Introduction to Practical Infrared Spectroscopy. Butterworth & Co. (Publishers) Ltd., pp 77-182.

Daveloose D, Linard A, Arfi T, Viret J and Christon R (1993). Simultaneous changes in lipid composition, fluidity and enzyme activity in piglet intestinal brush border membrane as affected by dietary polyunsaturated fatty acid deficiency. Biochim. Biophys. Acta 1166: 229-237.

Dev SB, Cho Kyun Rha and Walder F (1984). Secondary structural changes in globular protein induced by a surfactant: Fourier self-deconvolution of FT-IR spectra. J. Biomol. Struct. Dynam. 2: 431-442.

Dorr RT and Von Hoff DD (1994). Cancer Chemotherapy Handbook, 2nd ed., Appleton & Lange, pp 286-294.

Doyle LA (1993). Mechanisms of drug resistance in human lung cancer cells. Semin. Oncol. 20: 326-337.

Eastman A (1990). Activation of programmed cell death by anticancer agents: cisplatin as a model system. Cancer Cells 2: 275-280.

Emmelot P and van Hoven RP (1975). Phospholipid unsaturation and plasma membrane organization. Chemistry Physics Lipids 14: 236-246.

Fauvel J, Chap H, Roques V, Levy-Tolenado S and Douste-Blazy L (1986). Biochemical characterization of plasma membranes and intracellular membranes isolated from human platelets using Percoll gradient. Biochim. Biophys. Acta 856: 155-164.

Ferraro JR (1984). Vibrational Spectroscopy at High External Pressure. Academic Press, Inc. (London) Ltd.

Frei III E, Teicher BA, Holden SA, Cathcart KNS and Wang Y (1988). Preclinical studies and clinical correlation of the effect of alkylating dose. Cancer Res. 48: 6417-6423.

Fujiwara Y, Sugimoto Y, Kasahara K, Bungo M, Yamakido M, Tew KD and Sajio N (1990). Determinants of drug response in a cisplatin-resistant human lung cancer cell line. Jpn J Cancer Res. 81: 527-535.

Gaffin SL (1979). Rapid solubilization of human body tissues and tissue fluids for microdetermination of heavy metals. Clinical Toxicol. 15: 293-300.

De Gier J, Mandersloot JG and van Deenen LLM (1968). Lipid composition and permeability of liposomes. Biochim. Biophys. Acta 150: 666-675.

Ginsberg RJ, Kris MG and Armstrong JG (1993). Cancer of the lung. In: DeVita, Jr., VT, Hellman S and Rosenberg SA (eds.), Cancer: Principles & Practice of Oncology, 4th edition. J.B. Lippincott Co., Philadelphia, pp 673-680.

Goral J and Zichy V (1990). Fourier transform raman studies of material and compounds of biological importance. Spectrochimica Acta 46A: 253-275.

Grim WM III and Fateley WG (1984). Introduction to dispersive and interferometric infrared spectroscopy. In: Theophanides T (ed.), Fourier Transform Infrared Spectroscopy. D. Riedel Publis. Company, Holland, pp 25-42.

Hong WS, Saijo N, Sasaki Y, Minato K, Nakano H, Nakagawa K, Fujiwara Y, Nomura K and Twentyman PR. Establishment and characterization of cisplatin-resistant sublines of human lung cancer cell lines. Int. J. Cancer 41: 462-467.

Hospers GAP, Mulder NH and de Vris EGE (1988). Mechanisms of cellular resistance to cisplatin. Med. Oncol. & Tumor Pharmacoth. 5: 141-151.

Howell SB, Isonishi S, Christen RD, Andrews PA and Mann S (1991). Cellular pharmacologic strategies for overcoming drug resistance: potential application to regional therapy. Eur. J. Surg. Suppl. 561: 45-48.

Ismail AA, Mantsch HH & Wong PTT (1992) Aggregation of chymotrypsinogen: portrait by infrared spectroscopy. Biochim. Biophys. Acta 1121: 183-188.

Jakobsen RJ and Cornell DG (1986). FT-IR studies of langmuir-blodgett thin protein films: Albumin. Appl. Spectrosc. 40: 318-322.

Johnson SW, Ozols RF and Hamilton TC (1993). Mechanisms of drug resistance in ovarian cancer. Cancer Supplement 71: 644-649.

Karuhn RF and Berg RH (1984). Practical aspects of electrozone size analysis. In: Bedow K (ed), Particle Characterization in Technology. CPC Press vol I, pp 1-33.

Kates M (1986). Laboratory techniques in biochemistry and molecular biology. In: Technique of Lipidology: isolation, analysis and identification of lipids, 2nd edition. Elsevier, New York.

Kawai K, Kamatani N, Georges E and Ling V (1990). Identification of a membrane glycoprotein overexpressed in murine lymphoma sublines resistant to cis-diamminedichloroplatinum (II). J. Biol. Chem. 265: 13137-13142.

Kelland LR, Mistry P, Abel G, Freidlos F, Loh SY, Roberts JJ and Harrap KR (1992). Establishment and characterization of an in vitro model of acquired resistance to cisplatin in a human testicular nonseminomatous germ cell line. Cancer Res. 52: 1710-1716.

Kikuchi Y, Miyauchi M, Kizawa I, Oomori K and Kato K (1986). Establishment of a cisplatin-resistant human ovarian cancer cell line. J. Nat. Can. Inst. 77: 1181-1185.

Kimura E and Howell SB (1993). Analysis of the cytotoxic interaction between cisplatin and hyperthermia in a human ovarian carcinoma cell line. Cancer Chemother. Pharmacol. 32: 419-424.

Klausner RD, Kleinfeld AM, Hoover RL and Karnovsky MJ (1980). Lipid domains in membranes. J. Biol. Chem. 255: 1286-1295.

Lagarde M, Guichardant M, Menashi S and Crawford N (1982). The phospholipid and fatty acid composition of human platelet surface and intracellular membranes isolated by high voltage free flow electrophoresis. J. Biol. Chem. 257: 3100-3104.

Le Gal JM, Manfait M and Theophanides T (1991). Application of FTIR spectroscopy in structural studies of cells and bacteria. J. Molec. Struct. 242: 397-407.

Lyte M and Shinitzky M (1985). A special lipid mixture for membrane fluidization. Bioch. Biophys. Acta 812: 133-138.

Mann SC, Andrews PA and Howell SB (1988). Comparison of lipid content, surface membrane fluidity, and temperature dependence of cisplatin accumulation in sensitive and resistant human ovarian carcinoma cells. Anticancer Res. 8: 1211-1216.

Mann SC, Andrews PA and Howell SB (1990). Short term cis-diamminedichloroplatinum(II) accumulation in sensitive and resistant human ovarian carcinoma cells. Cancer Chemother. Pharmacol. 25: 236-240.

Mantsch HH, Wong PTT and Siminovitch DJ (1988). High pressure FT-IR spectra of aqueous systems: Application to biomembranes. Mikrochim. Acta [Wien] I: 167-169.

Mantsch HH and Wong PTT (1990). Pressure tuning vibrational spectroscopy: application to aqueous systems. Vibrational Spectrosc. 1: 151-157.

Marsh D and Smith ICP (1973). An interacting spin label study of the fluidizing and condensing effects of cholesterol on lecithin bilayer. Biochim. Biophys. Acta 298: 133-144.

May GL, Wright LC, Holmes KT, Williams PG Smith ICP, Wright PE, Fox RM and Mountford CE (1986). Assignment of methylene proton resonances in NMR spectra of embryonic and transformed cells to plasma membrane triglyceride. J. Biol. Chem. 261: 3048-3053.

Morikage T, Bungo M, Inomata M, Yoshida M, Ohmori T, Fujiwara Y, Nishio K and Sajio N (1991). Reversal of cisplatin resistance with amphotericin B in a non-small cell lung cancer cell line. Jpn. J. Cancer Res. 82: 747-751.

Mistry P, Kelland LR, Abel G, Sidhar S and Harrap KR (1991). The relationship between glutathione, glutathione-S-transferase and cytotoxicity of platinum drugs and melphalan in eight human ovarian carcinoma cell lines. Br. J. Cancer 64: 215-220.

Muga A, Surewicz WK, Wong PTT and Mantsch HH (1990). Structural studies with the uveopathogenic peptide M derived from retinal S-antigen. Biochem. 29: 2925-2930.

Murphy EJ and Horrocks LA (1993). Composition of the phospholipids and their fatty acids in the ROC-1 oligdendroglial cell line. Lipids 28: 67-71.

Nakagawa K, Yokota J, Wada M, Sasaki Y, Fujiwara Y, Sakai, Muramatsu M, Terasaki T, Tsunokawa Y, Terada M and Sajio N (1988). Levels of glutathione S transferase π m RNA in human lung cancer cell lines correlate with the resistance to cisplatin and carboplatin. Jpn. J. Cancer Res., 79: 301-304.

Nishikawa K, Newman RA, Murray L, Khokar AR and Rosenblum MG (1990). Detection of cellular platinum using the monoclonal antibody 1C1. Mol. Biother., vol 2, 235-241.

Nishio K, Sugimoto Y, Kasahara K, Fujiwara Y, Nishiwaki S and Fujiki H (1992). Increased phosphorylation of nuclear phosphoproteins in human lung-cancer cells resistant to cis-diamminedichloroplatinum (II). Int. J. Cancer 50: 438-442.

Oberc-Greenwood MA, Smith BH, Cooke C, Pepin C and Kornblith PL (1990). Selective cytoplasmatic and membrane changes induced by cisplatinum. J. Neuro-Oncol. 9: 191-199.

O'Dwyer PJ, Moyer JD, Suffness M and Harrison SD. (1994). Antitumor activity and biochemical effects of aphidocolin glycinate (NSC 303812) alone and in combination with cisplatin in vivo. Cancer Res. 54: 724-729.

Oldenburg J, Begg AC, van Hugt MJH, Ruevekamp M, Schornagel JH, Pinedo HM and Los G (1994). Characterization of resistance mechanisms to cisplatin in three sublines of the CC531 colon adenocarcinoma cell line in vitro. Cancer Res. 54: 487-493.

Okada K, Ozaki Y, Kawauchi K and Muraishi S (1990). The usefulness of infrared microspectroscopy for IR spectroscopic measurements of solid proteins. Appl. Spectrosc. 44: 1412-1414.

Owens, Jr A and Abeloff MD (1993). In: Calabresi P & Schein PS (eds.). Medical Oncology Basic Principles and Clinical Management of Cancer. McGraw-Hill, Inc., pp 593-624.

Ozols RF, O'Dwyer PJ and Hamilton TC (1993). Clinical reversal of drug resistance in ovarian cancer. Gynaecol. Oncol. 51: 90-96.

Pallares-Trujillo J, Domenech C,Grau-Oliete MR and Rivera-Fillat MP (1993). Role of cell cholesterol in modulating vincristine uptake and resistance. Intern. J. Cancer 55: 667-671.

Parker FS (1971). Application of Infrared Spectroscopy in Biochemistry, Biology and Medicine. Plenum, New York.

Philp RB, McIver DJL and Wong PTT (1990). Pressure distortion of an artificial membrane and the effect of ligand/protein binding. Biochim. Biophys. Acta 1021: 91-95.

Popovic P, Wong PTT, Goel R, Evans WK, Howell SB, Auersperg N and Stewart DJ (1992). Pressure tuning infrared spectroscopy of cisplatin sensitive vs resistant ovarian cancer cells. Proc. Am. Assoc. Cancer Res. 33: 464.

Popovic P, Teicher B, Wong PTT, Goel R and Stewart DJ (1993[a]) Pressure tuning infrared spectroscopy of EMT-6 tumor and its cyclophosphamide and cisplatin resistant variants. Proc. Am. Assoc. Cancer Res. 34: 405.

Popovic P, Wong PTT, Goel R, Evans WK, Howell SB and Stewart DJ (1993[b]). Pressure tuning infrared spectra of cisplatin sensitive and resistant human ovarian cancer cells exposed to cisplatin. Proc. Am. Assoc. Cancer Res. 34: 404.

Popovic P, Wong PTT, Kates M, Grewaal D, Goel R, Molepo JM and Stewart DJ (1994). Membrane fluidity in cisplatin resistant cells with low cisplatin uptake. Proc. Am. Assoc. Cancer Res. 35: 2626.

Rana APS, Misra S, Majumder GC and Ghosh A (1993). Phospholipid asymmetry of goat sperm plasma membrane during epididymal maturation. Biochim. Biophys. Acta 1210: 1-7.

Rapp E, Pater LJ, Willan A, Cormier Y, Murray N, Evans WK, Hodson DI, Clark DA, Feld R, Arnold AM, Ayoub JI, Wilson KS, Latreille J, Wierzbicki RF and Hill DP (1988). Chemotherapy can prolong survival in patients with advanced non-small-cell lung cancer, report of canadian multicenter randomized trial. J. Clinic. Oncol. 6: 633-641.

Reed E (1990). Cisplatin. In: Pinedo HM, Chabner BA and Longo DL (eds.). Cancer Chemotherapy and Biological Response Modifiers Annual II. Elsevier, Holland, pp 90-95.

Reed E and Kohn KW (1990). Platinum analogues. In: Chabner BA and Collins JM (eds.). Cancer Chemotherapy: Principles and Practice. Lippincott, Philadelphia, pp 465-490.

Reed E (1993). Platinum analogues. In: Rubin DK (ed.). Cancer: Principles & Practice of Oncology. J.B. Lippincott Co., Philadelphia, pp 390-395.

Richon VM, Schulte N and Eastman A (1987). Multiple mechanisms of resistance to cis-Diamminedichloroplatinum (II) in murine leukemia L1210 cells. Cancer Res. 47: 2056-2061.

Rigas B and Wong PTT (1992). Human colon adenocarcinoma cell lines display infrared spectroscopic features of malignant colon tissues. Cancer Res. 52: 84-88.

Rigas B, Morgello S, Goldman IS and Wong PTT (1990). Human colorectal cancers display abnormal Fourier-transform infrared spectra. Proc. Natl. Acad. Sci. USA 87: 8140-8144.

Robert J, Montaudon D and Hugues P (1983). Incorporation and metabolism of exogenous fatty acids by cultured normal and tumor glial cells. Biochim. et Biophys. Acta 752: 383-395.

Rosenburg B, Loretta van Camp, Trosko JE and Mansod VH (1969). Platinum compounds: a new class of potent antitumor agents. Nature 222: 385-386.

Ruiz-Gutierrez R, Vazquez CM and Quintero FJ (1992). Lipid composition, phospholipid profile and fatty acid of rat caecal mucosa. Biochim. Biophys. Acta 1128: 199-204.

Sanchez-Ruiz JM and Martinez-Carrion (1988). A Fourier-transform infrared spectroscopic study of the phosphoserine residues in hen egg phosvitin and ovalbumin. Biochemistry 27: 3338-3342.

Sanderman JR (1978). Regulation of membrane enzymes by lipids. Bioch. Biophys. Acta 515: 209-237.

Scanlon KJ, Kashani-Sabet M, Miyachi H, Sowers LC and Rossi J (1989). Molecular basis of cisplatin resistance in human carcinomas: model systems and patients. Anticancer Res. 9: 1301-1312.

Schmidt CF, Barenholz Y, Huang C and Thompson TE (1978). Monolayer coupling in sphingomyelin bilayer system. Nature 271: 275-277.

Schmidt W and Chaney SG (1993). Role of carrier ligand in platinum resistance of human carcinoma cell lines. Cancer Res. 53: 799-805.

Shie M, Kharitonenkov IG and Tikhonenko TI (1972). New possibilities of investigating nucleic acids and nucleoproteins in aqueous solutions by infrared spectroscopy. Nature 235: 386-388.

Shinitzky M (1984). Membrane fluidity in malignancy adversative and recuperative. Biochim. Biophys. Acta 738: 251-261.

Siminovitch DJ, Wong PTT and Mantsch HH (1987). Effects of cis and trans unsaturation on the structure of phospholipid bilayer: a high pressure infrared spectroscopy study. Biochemistry 26: 3277-3287.

Smith AL (1979). Applied Infrared Spectroscopy. John Wiley & Sons, New York, pp 24-40.

Soderberg M, Kristensson EK and Daliner G (1991). Fatty acid composition of brain phospholipids in aging and in Alzheimer's disease. Lipids 26: 421-426.

Stauffer JL (1992). In: Schroeder SA, Tierney, Jr LM, McPhee SJ, Papadakis MA and Krupp MA (eds.). Current Medical Diagnosis and Treatment. Appleton & Lange, pp 213-217.

Stewart DJ, Mikhael NZ, Nair RC, Kacew S, Montpetit V, Nanji A, Maroun JA and Howard K (1988). Platinum concentrations in human autopsy tumor samples. Amer. J. Clinic. Oncol. 11: 152-158.

Stewart DJ, Molepo JM, Eapen L, Montpetit VAJ, Goel R, Wong PTT, Popovic P, Taylor KD and Raaphorst GP (1993). Cisplatin and radiation in the treatment of tumors of the central nervous system: pharmacological considerations and results of early studies. Int. J. Radiation Oncology Biol. Phys. 28: 531-542.

Stewart DJ, Molepo JM, Green RM, Montpetit VAJ, Hugenholtz H, Lamothe A, Mikhael NZ, Redmond MD Gadia M and Goel R (1994). Factors affecting cisplatin concentrations in human surgical tumor specimens. In press.

Stryer L (1988). Biochemistry, 3rd ed. WH Freeman and Co., New York.

Susi H (1969). Infrared spectra of biological macromolecules and related systems. In: SN Timasheff & Fasman GD (eds.). Structure and Stability of Biological Macromolecules, pp 575-663.

Taylor KD, Goel R, Stewart DJ and Wong PTT (1992). Pressure tuning infrared spectroscopic study of cisplatin induces changes in phosphatidylserine model membrane. Proc. Am. Assoc. Cancer Res. 33: 448.

Taylor KD, Goel R, Stewart DJ and Wong PTT (1993). Pressure tuning infrared spectroscopic study of cisplatin induced changes in a phosphatidylcholine model membrane. Proc. Am. Assoc. Cancer Res. 34: 401.

Teicher BA, Holden SA, Kelley MJ, Shea TC, Cucchi CA, Rosowsky A, Henner WD and Frei III E (1987). Characterization of a human squamous carcinoma cell line resistant to cis-Diamminedichloroplatinum(II). Cancer Res. 47: 388-393.

Teicher BA, Herman TS, Holden SA, Wang Y, Pfeffer MR, Crawford JW and Frei III E (1990). Tumor resistance to alkylating agents conferred by mechanisms operative only in vivo. Science 247: 1457-1461.

Timmer-Bosscha H, Hospers GAP, Meijer C, Mulder NH, Muskiet FAI, Martini IA, Uges DRA and de Vris EGE (1989). Influence of docosahexaenoic acid on cisplatin resistance in a human small cell lung carcinoma cell line. J. Natl Cancer Inst. 81: 1069-1075.

Timmer-Bosscha H, Timmer A, Meijer C, de Vries EGE, de Jong B, Oosterhuis JW and Mulder NH (1993). Cisplatin resistance in vitro and in vivo in human embryonal carcinoma cells. Cancer Res. 53: 8707-8713.

Twentyman PR, Wright KA, Mistry P, Kelland LR and Murrer BA (1992). Sensitivity to novel platinum compounds of panels of human lung cancer cell lines with acquired and inherent resistance to cisplatin. Cancer Res. 52: 5674-5680.

van der Vijgh WJF and Klein I (1986). Protein binding of five platinum compounds. Cancer Chemoth. Pharmacol. 18: 129-132.

Warren GB, Houslay MD, Metcalfe JC and Birdsall NJM (1975). Cholesterol is excluded from the phospholipid annulus surrounding an active calcium transport protein. Nature 255: 684-687.

Willis R (1967). Pathology of Tumours, 4th ed. WB Saunders Company, Toronto.

Wong PTT, Moffatt DJ and Baudais FL (1985). Crystaline quartz as an internal calibrant for high pressure infrared spectroscopy. Appl. Spectrosc. 39: 733-735.

Wong PTT (1987). Vibrational spectroscopy under high pressure. In: JR Durig (ed.). Vibrational Spectra and Structure, vol 16, pp 357-445.

Wong PTT and Mantsch HH (1988). Reorientational and conformational ordering processes at elevated pressures in 1,2-dioleoyl phosphatidylcholine. Biophys. J. 54: 781-790.

Wong PTT and Mantsch HH (1989). FT-IR Spectroscopy: The detection of pressure-induced changes in the secondary structure of proteins. Biomolecular Spectroscopy 1057: 49-56.

Wong P'TT and Rigas B (1990). Infrared spectra of microtome sections of human colon tissues. Appl. Spectrosc. 44: 1715-1718.

Wong PTT, Cadrin M and French SW (1991). Distinctive infrared spectral features in liver tumor tissue of mice: evidence of structural modification at the molecular level. Experimental Molec. Pathol. 55: 269-284.

Wong PTT, Papavassiliou ED and Rigas B (1991). Phosphodiester stretching bands in the infrared spectra of human tissues and cultured cells. Appl. Spectrosc. 45: 1563-1567.

Wong PTT, Wong RK, Caputo TA, Godwin TA and Rigas B (1991). Infrared spectroscopy of exfoliated human cervical cells: Evidence of extensive structural changes during carcinogenesis. Proc. Natl. Acad. Sci. USA 88: 10988-10992.

Wong PTT (1992), private communication.

Wood R, Upreti GC and de Antueno RJ (1986). A comparison of lipids from liver and hepatoma subcellular membranes. Lipids 21: 292-300.

Yeagle PL, Young J and Rice D (1988). Effects of cholesterol on (Na^+,K^+)-ATPase ATP hydrolysing activity in bovine kidney. Biochemistry 27: 6449-6452.

Yeagle PL (1989). Lipid regulation of cell membrane structure and function. The FASEB J. 3: 1833-1842.

Zakim D and Wong PTT (1990). A high pressure, infrared spectroscopic study of the solvation of bilirubin in lipid bilayer. Biochemistry 29: 2003-2007.